Spinal Foraminal Stenosis

Novel methods and MRI in functional positions to improve diagnostics

John Hutchins

Department of Orthopaedics
Institute of Clinical Sciences
Sahlgrenska Academy,
University of Gothenburg

UNIVERSITY OF GOTHENBURG

2024

Layout:
Gudni Olafsson, GO Grafik AB, gudni@gografik.se

Illustrations cover and inlay:
Pontus Andersson, Pontus Art Production AB

Spinal Foraminal Stenosis
Novel methods and MRI in functional positions to improve diagnostics
© John Hutchins 2024
john.m.hutchins@gmail.com

ISBN 978-91-8069-643-2 (PRINT)
ISBN 978-91-8069-644-9 (PDF)

Printed in Borås, Sweden 2024
Printed by Stema Specialtryck AB

SVANENMÄRKET
Trycksak
3041 0234

A bend in the road is not the end of the road, unless you fail to make the turn

– Helen Keller

Abstract

Background

Symptomatic spinal foraminal stenosis can cause radiculopathy, sensory disruptions, and motor weaknesses in the extremities. These symptoms typically present intermittently and are closely linked to various functional positions or postures. The common diagnostic method includes a relaxed supine MRI, which brings up an important consideration: Could this relaxed position potentially mask pathologies that are otherwise evident in the postures or situations that trigger symptoms?

Aim

The primary objective was to investigate alterations in the properties of the spinal foramina and adjacent tissues with MRI during functional positions.

Methods

A systematic review of validated classification systems for spinal foraminal stenosis was carried out (Study I). In the next study, the lumbar spine was studied in eighty-nine patients using quantitative and qualitative means with Magnetic Resonance Imaging (MRI) under axial loading (Study II). Then, a new compression device for the cervical spine was introduced on ten healthy volunteers employing a simulated Spurling test, acquiring MR images in the provoked position (Study III). Furthermore, ten patients with intermittent arm radiculopathy and confirmed one or two level cervical foraminal stenosis were examined in a position of provoked arm pain during a simulated Spurling test (Study IV). In the last study, zero-echo-time (ZTE) sequences were acquired in both relaxed and provoked positions and were then integrated into Sectra® CT-based Micromotion Analysis (CTMA) for analysis (Study V).

Results

Three validated classification systems for spinal foraminal stenosis were identified. During axial loading of the lumbar spine a reduced foraminal area and altered foraminal gradings were found. The cervical compression device was successfully introduced on healthy volunteers, demonstrating the consistent application of a simulated Spurling test, further accomplishing a significant increase in the cervical angle and a decrease in the foraminal cross-distance in the axial image plane. In Study IV, all patients with cervical foraminal stenosis withstood the simulated Spurling test. In nine out of ten subjects, the test provoked concordant arm radiculopathy, resulting in significant increases in the foraminal gradings. Finally, the ZTE images were successfully employed in the CTMA, showing the most movement in C4/C5 levels compared with C5/C6 and C6/C7 during an ongoing Spurling test.

Conclusion

The identified validated classification systems proved to be usable in the three consecutive studies. MRI in functional positions offers a promising avenue for enhancing the diagnostic accuracy in diagnosing foraminal stenosis, particularly in patients with position-dependent symptoms. While there are challenges and limitations, the significant potential benefits in clinical practice warrant the continued exploration and refinement of these techniques.

Keywords: Spinal foraminal stenosis, Dynamic MRI, zero-echo-time MRI

ISBN 978-91-8069-643-2 (PRINT)
ISBN 978-91-8069-644-9 (PDF)

Sammanfattning på svenska

Bakgrund

Spinal foraminal stenos innebär en förträngning av den kanal som en specifik nervrot passerar igenom när den lämnar ryggmärgskanalen. Detta kan leda till utstrålande smärta (radikulopati) i denna nervs utbredningsområde. Den drabbade personen kan även uppleva känselstörningar och muskelsvaghet. Dessa symtom är tydligast när det påverkar nerver till armar eller ben, vilket innebär påverkan på nerver utspringande från halsryggen respektive ländryggen. Symtomen varierar ofta i intensitet över tid (intermittent), men är framför allt beroende av olika kroppslägen. Den vanliga diagnostiska metoden innebär en bild tagen i en liggande avslappnad position med MRI (Magnetic Resonance Imaging), vilket väcker en viktig fråga: skulle denna avslappnade position potentiellt kunna dölja förträngningar som annars kanske skulle vara uppenbara i de positioner eller situationer som utlöser symtomen?

Syfte

Det primära målet var att undersöka spinala foramina och angränsande vävnader med MRI i de positioner som utlöser symtom.

Metoder

En systematisk översikt av validerade klassificeringssystem för spinal foraminal stenos genomfördes. I ett nästa steg studerades ländryggen med kvantitativa och kvalitativa mått med MRI under axiell belastning. Sedan introducerades en ny kompressionsanordning för halsryggen på friska frivilliga. Ett simulerat Spurling test (kliniskt test) kunde göras i MR-maskinen och sedan kunde bilder tas i den provocerade positionen. Därefter undersöktes tio patienter med intermittent armsmärta och bekräftad cervikal foraminal stenos på en

eller två nivåer, i avlastat läge och i en position av provocerad armsmärta under ett simulerat Spurling test. I den sista studien analyserades Zero Echo Time (ZTE) sekvenser på samma patientgrupp som föregående studie och integrerade dem i Sectra® CT-based Micromotion Analysis (CTMA) för analys.

Resultat

Tre validerade klassificeringssystem för spinal foraminal stenos identifierades. Under axiell belastning av ländryggen identifierades en minskad foraminal area och förändring av klassificeringarna av foramina på gruppnivå. Den cervikala kompressionsanordningen introducerades sedan på friska frivilliga och kunde simulera ett Spurling test på ett konsekvent sätt. En ökning av vinkeln mellan kotorna i halsryggen uppmättes och en minskning av tväravståendet i foramina i det axiella bildplanet identifierades. I den följande studien med patienter med utstrålande armsmärta, tolererade alla det simulerade Spurling testet i MR-kameran. I 9/10 fall provocerade testet en armsmärta, som överensstämde med den smärta patienten vanligen led av. Högre grad av förträngning av foramina sågs vid klassificering av trängseln under provokation jämfört med bilder tagna i ett avslappnat läge. Slutligen påvisades mest rörelse i C4/C5-nivåerna jämfört med C5/C6 och C6/C7 under ett pågående Spurling test efter att ZTE-bilderna integrerats i CTMA.

Slutsats

De identifierade validerade klassifikationssystemen banade väg för användningen i de tre efterföljande studierna. MRI i funktionella positioner är en lovande väg för att förbättra diagnostisk noggrannhet för foraminal stenos, särskilt för patienter med positionsberoende symptom. Även om det finns utmaningar och begränsningar, motiverar de potentiella fördelarna fortsatt forskning och förfining av dessa tekniker.

List of papers

This thesis is based on the following studies, referred to in the text by their Roman numerals:

Hutchins J, Hebelka H, Lagerstrand K, Brisby H.

I. A systematic review of validated classification systems for cervical and lumbar spinal foraminal stenosis based on magnetic resonance imaging.

Eur Spine J. 2022 Jun;31(6):1358-1369. doi: 10.1007/s00586-022-07147-5. Epub 2022 Mar 28. PMID: 35347421.

Hebelka H, Rydberg N, Hutchins J, Lagerstrand K, Brisby H.

II. Axial Loading during MRI Induces Lumbar Foraminal Area Changes and Has the Potential to Improve Diagnostics of Nerve Root Compromise.

J Clin Med. 2022 Apr 11;11(8):2122. doi: 10.3390/jcm11082122. PMID: 35456215; PMCID: PMC9029659.

Hutchins J, Lagerstrand K, Stävlid E, Svensson PA, Rennerfelt K, Hebelka H, Brisby H.

III. MRI evaluation of foraminal changes in the cervical spine with assistance of a novel compression device.

Sci Rep. 2023 Jul 17;13(1):11508. doi: 10.1038/s41598-023-38401-5. PMID: 37460649; PMCID: PMC10352332.

Hutchins J, Hebelka H, Svensson PA, Myklebust TÅ, Lagerstrand K, Brisby H.

IV. Cervical Foraminal Changes in Patients with Intermittent Arm Radiculopathy Studied with a New MRI-Compatible Compression Device.

J Clin Med. 2023 Oct 12;12(20):6493. doi: 10.3390/jcm12206493. PMID: 37892631; PMCID: PMC10607115.

Hutchins J, Lagerstrand K, Hebelka H, Palmér E, Brisby H.

V. Evaluation of cervical vertebral motions and foraminal changes during Spurling test using zero echo time MRI and CT Micromotion Analysis.

Accepted. Spine. 2024 Apr 1.

Contents

Abbreviations

AI	Artificial Intelligence
ALL	Anterior Longitudinal Ligament
CFS	Cervical Foraminal Stenosis
CI	Confidence Interval
EQ-5D 5L	EuroQol 5 Dimension
ICR	Instantaneous Center of Rotation
IVD	Intervertebral Disc
LBP	Low Back Pain
LFS	Lumbar Foraminal Stenosis
NDI	Neck Disability Index
PLL	Posterior Longitudinal Ligament
RF	Radio Frequency
ROM	Range Of Motion
SLR	Straight Leg Raise
SNR	Signal to Noise Ratio
TE	Time to Echo
TR	Time to Repetition
VAS	Visual Analog Scale
ZTE	Zero Echo Time

Devices and analysis software

Dynawell®	Dynawell Diagnostics Inc., 1452 Via Merano St Henderson, NV 89052, USA is a compression device for the lumbar spine.
DMRICS	Dynamic MRI Compression System is the prototype used for compressional forces in the cervical spine.
Sectra® CTMA	CT-Based Micromotion Analysis by Sectra AB, Teknikringen 20, 583 30 Linköping, Sweden is a software for measuring micromotions between image sets.

Chapter 1

Introduction

The spinal foramen is defined as the passage through which nerve roots extend from the spinal cord and out the side of the spinal column.[1] It is sculpted by the side components of two adjacent vertebrae, a disc, and the encompassing facet joints and ligaments that bind them. This path of the departing nerve is nestled within a vertebral motion segment. Over time, these segments degenerate, leading to anatomical shifts caused by diminished or protruding discs, enlarged facet joints, and ligaments.[2] Given that these structures shape the foramen, any alterations can jeopardize the space for emerging nerve roots, potentially causing foraminal stenosis, with the possibility of nerve root compression (Figure 1).

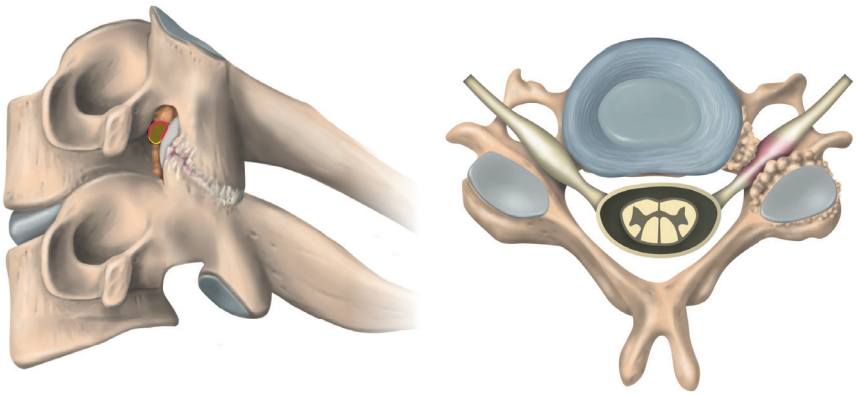

Figure 1 The oblique view to the left depicts cervical foraminal stenosis, with the nerve emerging from the foramina towards the viewer. The narrowed foramen is pressing against the nerve, highlighted in red. To the right, an axial perspective reveals the constricted foramen squeezing the nerve, which is subtly marked in pink.

If a nerve root becomes trapped in the foramina, this entrapment can cause pain and neurological symptoms related to the specific motor and sensory functions they correspond to.[3,4] If the foraminal stenosis occurs in the cervical region, it can give rise to symptoms in the arms in the form of sensory disturbances, muscle weakness, and/or radiculating arm pain.[5] Similarly, if a lumbar foramina is affected, this can give rise to symptoms in the lower limbs.[6] Initially, patients with

foraminal stenosis are treated using conservative methods, such as pain-relieving medications and physiotherapy.[7] If these measures do not yield satisfactory results, surgery may be considered. Surgical options include decompression of the nerve root(s) affected, sometimes with the addition of a fusion or in some cases disc prothesis.[8] Numerous patients experience intermittent symptoms, which manifest in various postural or neck/spine positions, commonly while sitting or standing.[9] Yet there is a problem of discrepancy between MRI findings and clinical presentation, especially in patients who have more than one suspected foraminal stenosis.[10] This may be because the neck or lumbar spine is examined in the MRI in a relaxed supine position and not in a functional position in which the pain is usually is aggravated. Therefore, the overall aim of this thesis is to address this problem by acquiring MRI in positions in which the patients experience the pain and thereby explore possible diagnostic enhancements.

Chapter 2

Background

Core spinal functions

The spinal column serves as a protective shield for the spinal cord and spinal nerve roots while providing essential structural support for the head down to the buttocks. The whole spine is endowed with facet joints and intervertebral discs (IVDs) that grant the required flexibility for maintaining proper posture.[11] The cervical spine plays a pivotal role in human anatomy enabling a wide range of motion for the head. The thoracic spine is connected to consecutive ribs and constitutes the posterior structure of the rib cage. This section of the spine is the most rigid and stable part.[12] The lumbar spine serves as the foundation of the spinal column. While it offers less range of motion than the cervical spine but more than the thoracic spine, it has similar anatomic elements but in slightly different shapes in larger sizes.[13]

Segment differences

The spine consists of seven cervical, 12 thoracic and five lumbar vertebrae [14] (Figure 2). Distinct from other sections, the first two segments of the cervical spine possess uniquely shaped vertebrae and joints. They do not have the IVDs that the subsequent segments do. The joint that connects the skull to the spine, the occiput-atlas joint, facilitates the nodding motion of the head. Directly below this, the atlanto-axial joint is responsible for about 40% of the neck's rotational movement.[12] While a more consistent cervical anatomy is evident from the third vertebra downwards, this part is often referred to as the subaxial segments.

The thoracic spine has distinct anatomical features.[15] It consists of 12 vertebrae and makes up the typical kyphotic curvature with the apex at the higher levels. The thoracic spine is connected to pairs of ribs, one on each side of each vertebrae. The vertebrae have a

substantially longer spinous processes with a steeper posteroinferior angle than that of the vertebrae in the subaxial spine region, and the pedicles are generally narrow and oval shaped.

The lumbar spine represents the sturdy foundation that blend into the formation of the sacral bone, which in turn interconnects with the pelvis.[13] There are typically five lumbar vertebral bodies that help create a lordosis that, together with the thoracic kyphosis, creates a harmonic S-curve.

Intervertebral discs

The human spine owes much of its flexibility and shock-absorbing capacity to the IVDs (Figure 3). These discs, situated between each vertebral body, serve as pivotal connectors, cushioning agents, and stabilizers, ensuring that the spine can withstand various stresses and strains.[16] Diving deeper into the anatomy, IVDs are composed of the annulus

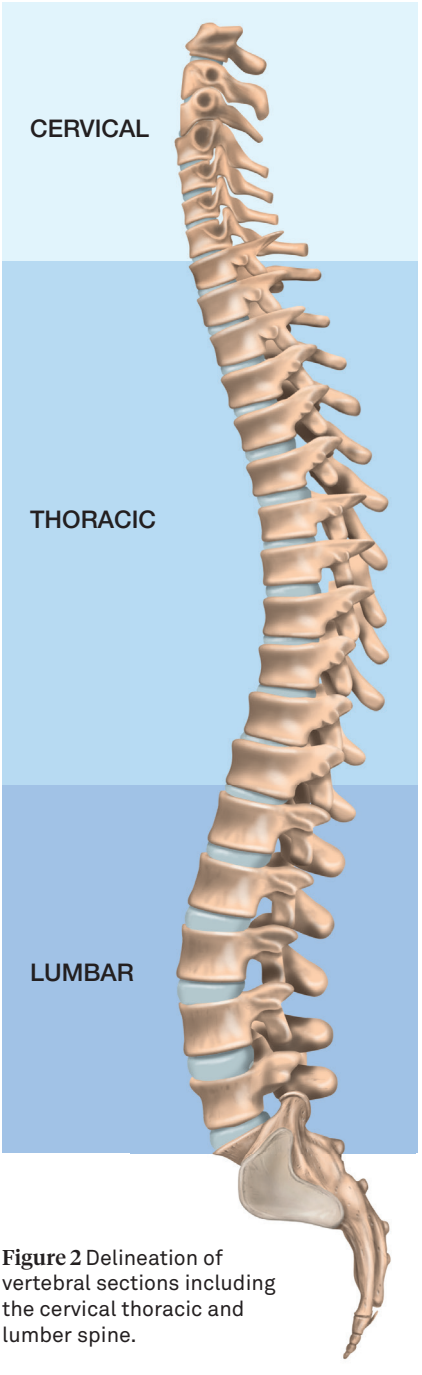

Figure 2 Delineation of vertebral sections including the cervical thoracic and lumber spine.

fibrosus and nucleus pulposus.[16] The nucleus pulposus, a gel-like center, gives the disc its shock-absorbing capabilities. It behaves much like a water balloon, uniformly distributing the compressive forces applied to the spine during activities such as walking or lifting.[17] Encasing this nucleus is the annulus fibrosus, a multi-layered, fibrocartilaginous ring that provides structural integrity to the disc. It resists tension and contains the nucleus, preventing it from herniating or bulging outwards.[18] A noteworthy feature is that the disc's posterior section is enveloped by the posterior longitudinal ligament.[19] Due to the annulus fibrosus's unique shape, the nucleus positions itself slightly towards the rear.[19] The exterior of the annulus fibrosus is vascular, whereas most of the annulus and the nucleus are devoid of blood vessels. However, it derives its nourishment via diffusion from blood vessels within the neighboring vertebrae through the endplates.[18] Both the annulus's outermost region and the posterior longitudinal ligament possess nerve endings sensitive to pain.

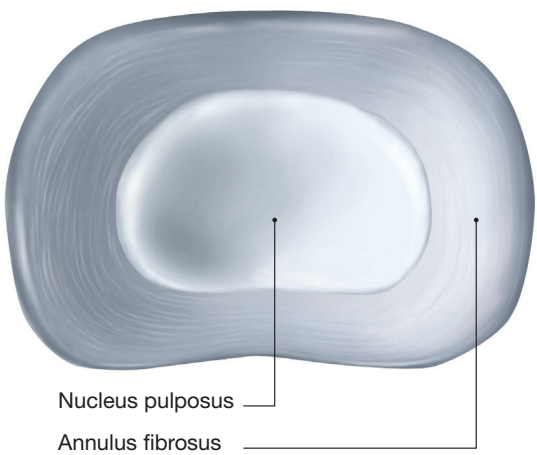

Figure 3 Illustration of an intervertebral disc in the axial plane.

The anatomy and function of the IVDs vary slightly based on their position within the spine. In the cervical region, the discs are smaller and thinner, tailored to support the neck's wide range of motion while bearing the weight of the head.[17,20] This contrasts with the thoracic spine's discs, which are relatively thin and more rigid. Their relative inflexibility aligns with the thoracic spine's more limited mobility, reinforced by the rib cage's presence, which ensures added stability and protection for some of the body's vital organs. Moving down to the lumbar region, the discs are notably thicker and larger. This is a response to the higher mechanical loads placed on the lower back. Their robust structure balances the demands of strength and mobility, a crucial combination for daily activities such as lifting, bending, and twisting. In essence, the IVDs are intrinsic to the spine's architecture and function, providing both mobility and stability across life's various physical demands.

Ligaments

The human spine, a marvel of biomechanical engineering, is bolstered and stabilized by a network of integral ligaments[21] (Figure 4). These ligaments not only provide foundational support but also guide and limit the spine's range of motion, ensuring its functional integrity.[22]

Starting from the front of the spine, the anterior longitudinal ligament (ALL) runs vertically along the anterior surface of the vertebral bodies and IVDs. Its primary role is to limit the spine's extension or backward bending. Behind the vertebral bodies, but still anterior to the spinal canal, lies the posterior longitudinal ligament (PLL). This ligament primarily acts as a check against forward bending or flexion and offers additional protection against posterior disc herniations. Inside the spinal canal, connecting the laminae of adjacent vertebrae, is the elastic ligamentum flavum. Beyond lending support, this ligament plays an accessory role in maintaining our upright posture and aids in

realigning the spine post-flexion.[23] Between the protruding spinous processes of each vertebra, we find the interspinous ligaments. Their function is straightforward, to limit the amount of flexion and serve as anchor points for spinal muscles. Running along the tips of the spinous processes from the base of the neck to the sacrum is the supraspinous ligament, another guardian against excessive spinal flexion. On the lateral aspects of the vertebrae, connecting the transverse processes, are the intertransverse ligaments. These ligaments aid in resisting the spine's lateral flexion or side-to-side bending. Each vertebra is also equipped with capsular ligaments that envelop the facet joints. These ligaments are important in limiting over-rotation and excessive flexion of the spine. Finally, in the cervical region, there is the nuchal ligament, extending from the skull's external occipital protuberance down to the seventh cervical vertebra. This ligament, unique to the neck, offers a posterior midline anchor for neck muscles and restricts excessive cervical flexion.

These ligaments, harmoniously interwoven with the spine's muscles and bony architecture, participate in its stability and flexibility. Their collaborative function is a testament to the intricate design and functionality of the human spine.[20]

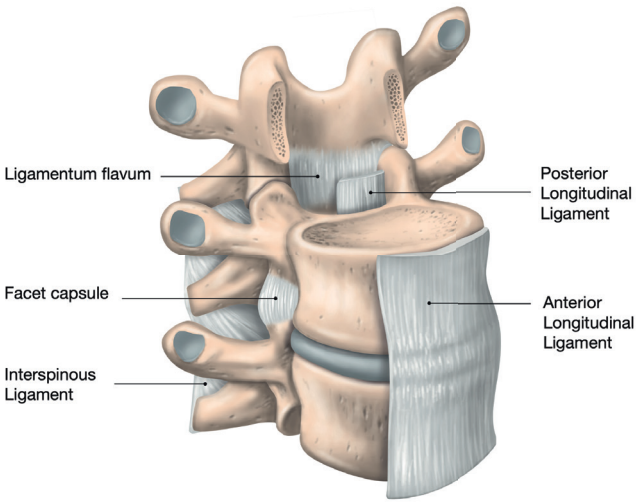

Figure 4
Illustration of crucial spinal ligaments, aiding in the stability and integrity of the spinal cord and nerve roots.

Facet joints

Facet joints play a significant role in the spine (Figure 5). They not only guide movements but are also renowned for their inherent flexibility, a trait attributed to their relatively loose joint capsules. Their intrinsic design and surrounding bone are abundant in sensory nerve endings.[24]

The first and second cervical vertebrae are unique in their shapes as discussed above.[25] The subaxial vertebrae have a more uniform anatomy. They are also home to the uncovertebral joints, which are uniquely situated at the rear corners of the intervertebral bodies.[26] These joints inhibit movements in the lateral direction but allow for stable flexion and extension.

In the thoracic spine, there are special facet joints where the ribs connect to the corresponding vertebra. Each link represents a type of facet joint called a demifacet.[15] The facet joints connecting the adjacent vertebrae have a particular angle, tilted anteroposteriorly compared with the rest of the spine.[15]

In the lumbar spine, the facet joints gradually twist from the sharp anteroposterior angle in the thoracic spine to a mediolateral angle.[27] There are indications that there is a variability in the angle between the joints at the same level. This asymmetry is more prevalent at the lower levels (L4/L5 and L5/S1) and may be a contributor to the predominance of degeneration at these levels.[28]

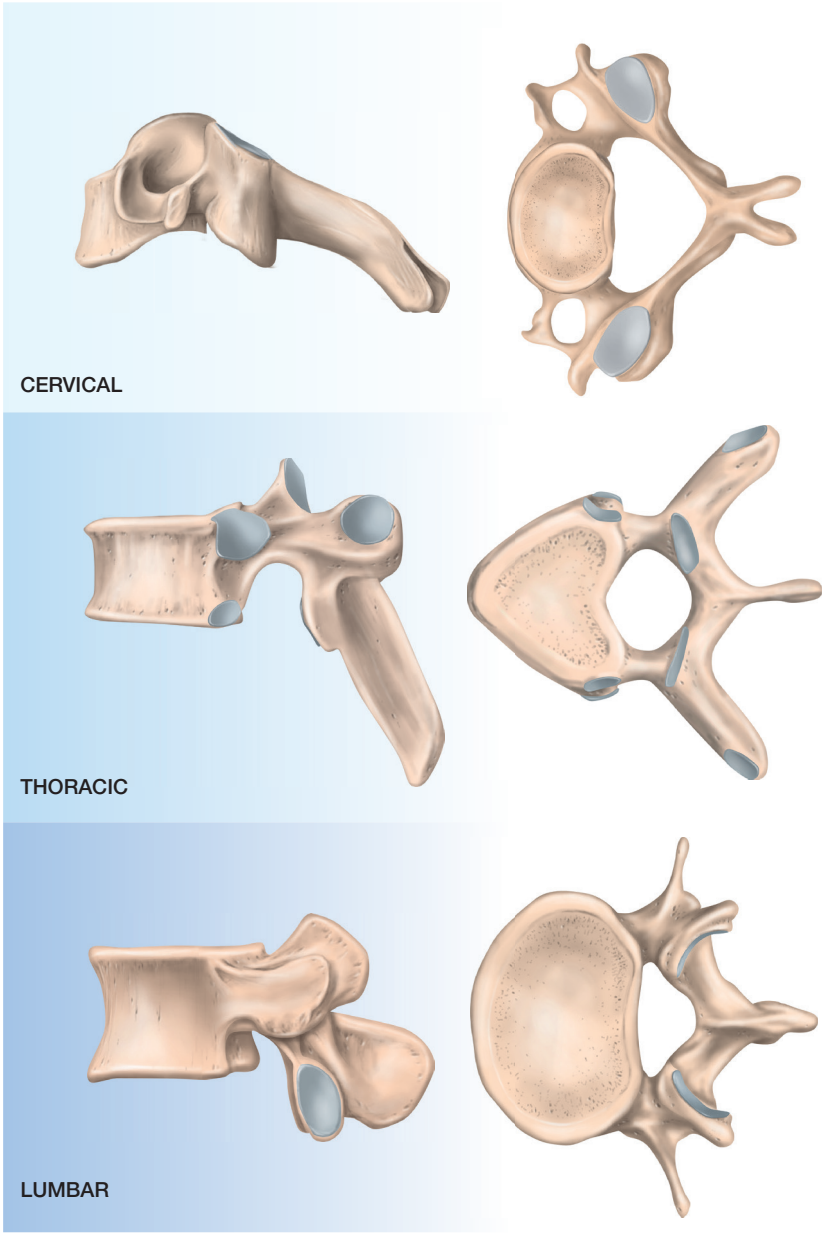

Figure 5 Illustrations of a typical cervical, thoracic, and lumbar vertebra. The gray areas represent articular surfaces.

The foramen and spinal nerves

The spinal foramen serves as the passage through which nerve roots extend from the spinal canal and reach the outside of the spinal column.[1] It is sculpted by the side components of two adjacent vertebrae, a disc, and the encompassing facet joints and ligaments that bind them[29] (Figure 6). Eight spinal nerves originate from the cervical, twelve from the thoracic, and five from the lumbar regions (Figure 7). Each nerve passes through its dedicated intervertebral foramina. The cervical nerves provide innervation to the neck, shoulders, and arms, and the back branches of these nerves, known as the dorsal rami, extend to the facet joints and the muscles lining the back of the neck.[29] In the thoracic spine, the exiting nerve roots primarily have a sensory function in the skin surrounding the torso.[15] In the lumbar spine, five pairs of nerve roots exit the spinal canal and are responsible for the innervation of the legs.[12]

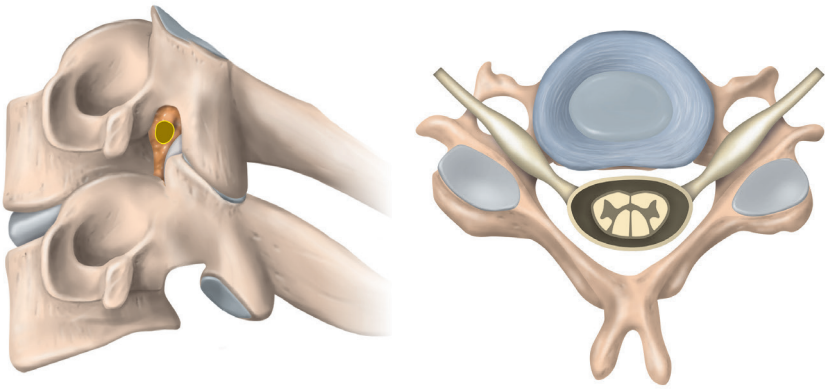

Figure 6 To the left, a cervical motion segment illustrating the foramina and nerve root exiting towards the observer. To the right an axial view of a cervical disc level and the bilateral foramina with corresponding exiting nerve roots.

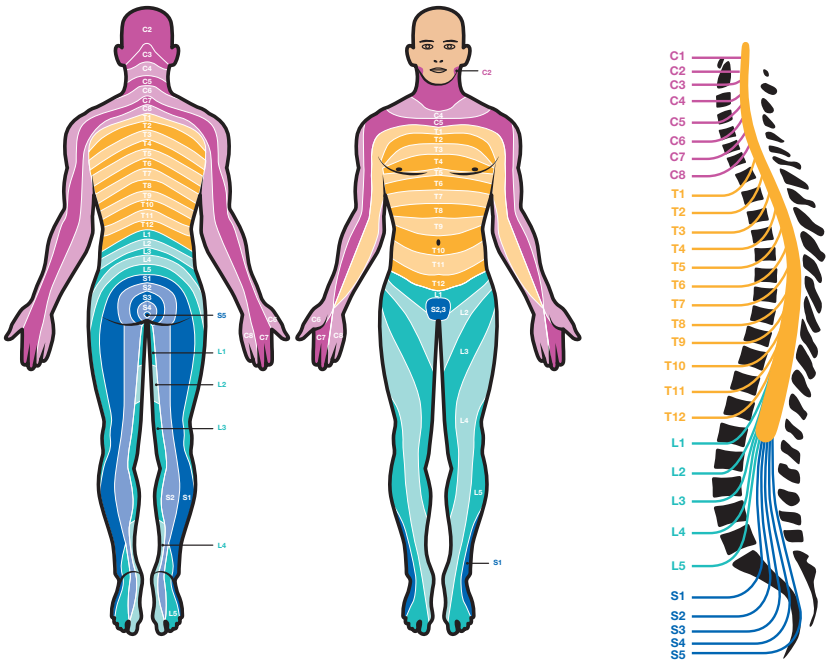

Figure 7 Dermatomes illustrated with different colors for clarity between different levels.

Stability and mobility

The cervical region of the spine boasts the greatest flexibility and range of motion, followed by the lumbar and then the thoracic spine.[20,30,31] The spine's stability is anchored by three interconnected systems: passive, active, and neural.[11]

The passive system pertains to the physical structure of the spine, including facet joints, uncovertebral joints, and ligaments.[20] It primarily offers stability during extreme ranges of motion and conveys information about the spine's position and movements to the neural system through special sensors called proprioceptive receptors.[11]

The neural system then evaluates this information to determine the necessary muscle action and contractions. Studies have found that the spine's passive structures can support 20–25% of an average head's weight, highlighting the significant role cervical muscles play in providing mechanical support.[25]

The active system relies on an interconnected matrix of muscles and tendons. This matrix envelops the spine, offering a robust foundation that guarantees stability. Beginning in the cervical region, the deep neck flexors such as the longus capitis and longus colli are essential for neck stability. The larger muscles, such as the sternocleidomastoid and the trapezius, provide broader neck movements and postural control.[21] Descending into the thoracic region, the erector spinae muscles, including the iliocostalis, longissimus, and spinalis, run vertically along the spine and facilitate trunk extension, lateral flexion, and rotation.[12] Intersegmental muscles, such as the multifidus and rotatores, span a few vertebral segments and play an important role in segmental stability, especially in the lumbar region.[17] The lumbar area also boasts the quadratus lumborum, which aids in lateral trunk flexion and stabilizing the lower spine.[17] Anteriorly, the abdominal musculature, including the rectus abdominis, obliques, and transversus abdominis, contribute significantly to spinal stability, intra-abdominal pressure regulation, and movement.[32] These muscles, in synergy, provide dynamic stability to the spine, allowing for a vast range of motions while safeguarding spinal structures from undue stress.

The spine's neural system plays an essential role in ensuring mechanical support and stability. This complex network is intricately involved in sensing positional changes and coordinating muscular responses to maintain spinal equilibrium. The proprioceptive information from facet joint capsules, IVDs, and ligaments is conveyed to the central nervous system, which then processes these data to modulate muscle activity and postural adjustments appropriately. For instance, the

mechanoreceptors in the ligaments and facet joints contribute to the spine's ability to detect motion and adjust its position in response to external forces.[11] Furthermore, the intrinsic and extrinsic muscles of the spine, under the control of the neural system, function in harmony to provide dynamic stabilization, ensuring that the alignment and movement of the vertebral column are both fluid and protected.[33] Disruptions or abnormalities within this neural control can compromise spinal stability, emphasizing the neural system's significance in biomechanical integrity.[34]

The range of motion (ROM) of the spine varies based on its segment. The ROM for each section is usually expressed in terms of flexion (bending forward), extension (bending backward), lateral flexion (bending to the side), and rotation (twisting). Typical ranges for the major sections of the spine are presented in Table 1. Rotation is notably limited in the lumbar spine, which is built for stability rather than rotation. The sacral and coccygeal sections are largely fused in adults and, thus, have limited to no motion.

Table 1 Spinal range of motion in different spinal segments.

Cervical Spine [20]	Thoracic Spine [30]	Lumbar Spine [31]
Flexion: 45–90°	Flexion: 20–45°	Flexion: 40–60°
Extension: 45–90°	Extension: 25–45°	Extension: 15–35°
Lateral Flexion: 20–45°	Lateral Flexion: 25–40°	Lateral Flexion: 15–25°
Rotation: 70–90°	Rotation: 35–50°	Rotation: 3–18°

Cervical subaxial motion properties

The subaxial cervical spine, comprising vertebrae C3 to C7, serves as a supportive column. In its design, the vertebral bodies' endplates exhibit a subtle sagittal curvature characterized by a forward-pro-

jecting edge that descends toward the lower adjacent vertebra. This anatomical configuration results in the IVDs being positioned at a slight angle relative to the longitudinal axis of the vertebral bodies, a feature that enhances the spine's ability to bend forward (flexion) and backward (extension) within the sagittal plane.[35] The cervical intervertebral joints, akin to saddles, allow for complex movement patterns. They are designed such that axial rotation and lateral flexion are inherently interlinked, suggesting a coordinated ballet of movement with each turn of the head or bend of the neck.[25] Within this subaxial region, the axial rotation is on average 6 degrees at each level, while flexion and extension fluctuate between 10 and 16 degrees.[35] This design ensures both stability and flexibility, a remarkable combination for the demands placed on our necks daily.

A groundbreaking study by Van Mameren,[36] employing high-speed cineradiographs, shifted the perspective on cervical motion studies. It was revealed that the maximum motion of a cervical segment is not just its end-to-end movement; rather, it varies throughout the motion process. Additionally, the range of movement changes based on the direction and over time. This underscores that there is no fixed "normal" range, emphasizing the variable nature of neck movements.

Historically, researchers believed there was a specific, standard order for the movement of individual cervical vertebrae. Buonocore et al. [37] described this movement as a sequential and harmonious separation of the vertebrae during flexion. However, this idealized motion pattern is more intricate and not as straightforward as earlier described. Van Mameren's analysis of the cervical spine's movement in ten individuals highlighted the complexity of the motion. Flexion starts in the lower cervical spine (C4/C7) and then progresses upwards, with C6/C7 being pivotal in both initiating and concluding the flexion. Conversely, extension starts in the same region (C4/C7) but the sequence of individual vertebrae contribution varies. Notably, individuals consistently exhibit this movement pattern, especially in the lower cervical spine.

The mid-cervical levels (C2/C4) are the most variable.

The instantaneous center of rotation (ICR) is the center around which a vertebra rotates. Using lateral radiographs, one can determine this center. Penning[38] first provided normative data about the ICRs, noting varied locations depending on the cervical segment. However, his data had limitations in accuracy and representation.[39] Subsequent studies improved these methods and, using a sample of 40 normal individuals, accurately mapped the ICR locations.[40] While there is debate about ICR validity, studies have emphasized its reliability.[41] Generally, from top to bottom, ICRs are positioned progressively higher, with their placement influenced by the height of the articular pillars[42] (see Figure 8).

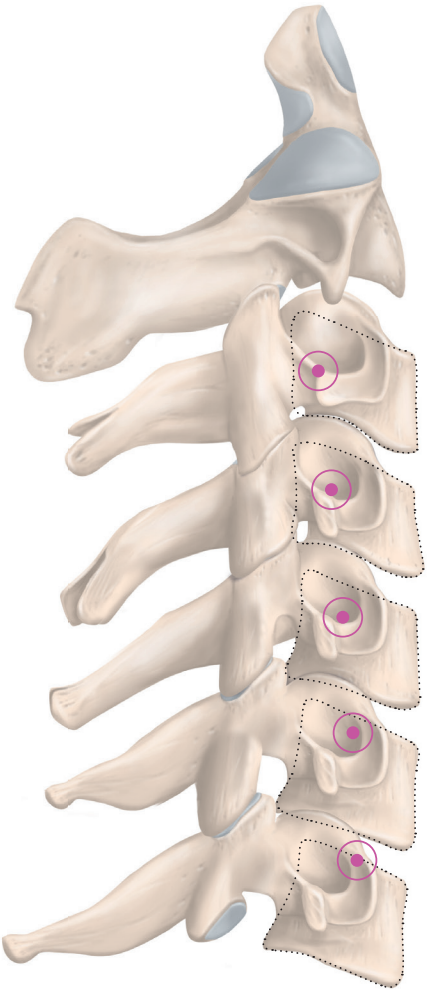

Figure 8 Schematic location of ICR

Degeneration of the spine

Degeneration of the spine can be a source of pain and disability.[43] The limits of various motions are an important aspect of spinal disability, depending on which components of the spine that are affected. The process of degeneration can involve IVDs, facet joints, ligaments, and the vertebrae themselves.[44]

As IVDs degenerate, they lose water content, leading to decreased disc height. As a consequence of the reduced water content, the disc height and the space between the vertebrae decreases and this may limit flexion and extension motions because the vertebrae are closer together.[18] Facet joints guide the motion between adjacent vertebrae. As they degenerate, they can become arthritic and develop bone spurs (osteophytes). This can lead to limited rotation and lateral flexion due to pain or mechanical obstruction from the bone spurs. Additionally, the joint capsule can become thickened and fibrotic, further restricting movement.[24] Ligaments, such as the ligamentum flavum, can thicken and calcify as they degenerate. This can impinge on the spinal canal or neural foramina, potentially compressing nerve roots. This does not necessarily limit motion directly, but can cause pain during certain motions, effectively reducing mobility.[44] As the body tries to stabilize an unstable segment, it may produce bone spurs. These can physically block or restrict movements, especially if they form in or around the facet joints or vertebral bodies.[45] In some cases, degeneration can cause one vertebra to slide forward over the one below it, called spondylolisthesis.[46] This can limit extension motion and potentially cause neural compression. Muscles may become less flexible or weaker due to pain inhibition or disuse, secondary to the degenerative changes. This can limit all motions to varying degrees.[47] The process of degeneration is complex. Genetic factors and possible trauma and infections are aspects also important to take into consideration when striving to understand the degenerative process.[2] Spinal degeneration often leads to foraminal stenosis in both the cervical and lumbar regions of the spine. This condition arises when the foraminal canal, the transitional bony tunnel through which nerve roots exit the spine, becomes narrowed due to degenerative changes.[1] The degenerative process, as outlined, results in several morphological changes, for example, the loss of disc height, development of osteophytes, thickening of ligaments, and potential spondylolisthesis, all of which can significantly contribute to the narrowing of the foraminal canals. Consequently, this narrowing can compress

the nerve roots passing through, causing pain and limiting the individual.[2] The onset of foraminal stenosis due to spinal degeneration underscores the intricate and multifaceted nature of spinal disorders and the complex interplay between various spinal components and pathologies.

Chapter 3

Foraminal Stenosis

Cervical radiculopathy as a spinal pathology was first recognized in 1817 and the pathology has successively been clarified in the years since.[48] The progression of degenerative changes in the cervical spine is usually revealed in the middle-aged population and continues with advancing age. The prevalence of symptomatic cervical foraminal stenosis (CFS) is in the range of 107–580/100,000 individuals.[49] The most prevalent level of disc degeneration and spondylosis is C5/C6 followed by C6/C7 and lastly C4/C5.[50] A research group studied 497 asymptomatic individuals and found that 20% had disc degeneration and fewer than 5% had radiological findings of foraminal stenosis at the age of 30 years. In the age group over 60 years of age they found that over 80% had disc degeneration and 15% had foraminal stenosis.[51] The symptoms of spinal nerve root impingement can be very aggravating and give rise to high patient interaction with the health care system and is further responsible for significant health care costs.[52]

Foraminal stenosis in the lumbar spine is one of the most common causes of leg sciatica.[9] The symptoms were described over a thousand years ago, but the pathology behind lumbar foraminal stenosis was first comprehensively described in 1927 by Professor V. Putti.[53] Lumbar foraminal stenosis is now known to be a common cause of leg sciatica with a prevalence of 8–11% and is more often found in middle-aged or older individuals. The most prevalent level for LFS is L5/S1 followed by L4/L5 and then L3/L4.[54]

Symptoms of foraminal stenosis

The nerve roots that pass through the foramina are integral components of the body's neural network, responsible for transmitting signals between the spinal cord and the rest of the body.[55] When these nerve roots become compressed or irritated due to the narrowing of the foramina, it can lead to a cascade of symptoms that are typically classified into three primary categories: radicular pain, motor weakness, and sensory disturbances.[9,55]

Radiculating pain: Perhaps the most prominent symptom of foraminal stenosis is radiculating pain, often described as a sharp, shooting, or burning sensation that follows the path of the affected nerve.[56] This pain is typically unilateral, radiating from the site of the stenosis into the extremities, often following a dermatomal pattern. It is the direct result of nerve root compression and can be exacerbated by certain movements or postures that further narrow the foramina or stretch the affected nerve.[57] Please see Figure 7 for an illustration of the dermatomes.

Motor weakness: The nerve roots also play a crucial role in motor function, carrying signals from the brain to various muscles. Compression of these nerve roots can hinder these signals, leading to muscle weakness in the regions served by the affected nerve.[55] Over time, if left untreated, this can result in muscle atrophy and decreased functional ability.

Sensory disturbances: Sensory disturbances in foraminal stenosis patients manifest as numbness, tingling, or a "pins and needles" sensation.[55] Like radicular pain, these disturbances often follow a dermatomal pattern. They arise because the nerve roots, in addition to transmitting motor signals, are responsible for conveying sensory information from the body back to the brain. Compression or irritation can disrupt this flow of information, leading to these sensory anomalies.

Foraminal stenosis is most common in the cervical and lumbar spine and uncommon at the thoracic levels. This is because the rib cage provides rigid stability, making degeneration less likely to occur in this region of the spine. If thoracic foraminal stenosis is diagnosed, the symptoms are most likely to be numbness and/or radiating pain in the corresponding dermatome half-way around the chest. Surgical treatment is rarely used in these cases.[58]

Radiculopathy deriving from the neck or lumbar spine may also be associated with neck or low back pain (LBP). This may be connected to the release of neuropeptides from battered nerve roots.[9] Both the cervical spine and lumbar spine are prone to degeneration and the development of foraminal stenosis. In the cervical spine, this is due to its more flexible motion segments, and in the lumbar spine, partly because of relatively flexible motion segments, but also because it is affected by the heavy load it needs to withstand.[49,54] Please find the specific nerve functions presented in Tables 2 and 3;[59] also, see an illustration of the dermatomes in Figure 7.

Table 2 Cervical nerve root motor and sensory functions, including reflexes.

Disc level	Root	Motor	Sensory	Reflex
C3/C4	C4	Longus capitis, longus colli, scalene muscles and levator scapulae	Neck, above the clavicle and upper region of chest	-
C4/C5	C5	Deltoid, supra- and infraspinatus	Lower neck, upper region of chest, deltoids, and anterior middle parts of the arms	Biceps/supinator reflex
C5/C6	C6	Biceps, brachioradialis, and wrist extensors	Lower neck, lateral aspects of the arms and thumb	Supinator/Biceps reflex
C6/C7	C7	Triceps, wrist flexors, and finger extensors	Posterior part of the arms and middle fingers	Triceps reflex
C7/Th1	C8	Thumb flexors, abductors, and hand intrinsic muscles	Medial aspects of the arms, predominantly the 5th finger	-

Table 3 Lumbar nerve root motor and sensory function including reflexes.

Disc level	Root	Motor	Sensory	Reflex
L3/L4	L3	Leg adductors, ileopsoas and more	Anteriomedial aspects of the thigh	-
L4/L5	L4	Knee extenders	Anterior aspect of thigh and medial part of lower leg and foot	Patellar
L5/S1	L5	Long toe extensors	Lateral aspect of thigh, anterior part of lower leg and middle dorsal aspect of foot	-
S1/S2	S1	Ankle plantar flexors	Back of the calf, lateral part of foot	Achilles

Peripheral nerve fibers

The peripheral nerves are classified according to their different macroscopic and functional properties;[60] please see Table 4, below.

Table 4 Peripheral nerve root types.

Fiber type	Diameter (µm)	Velocity (m/s)	Myelination	Primary Function
Aα	13–20	80–120	Myelinated	Motor to skeletal muscles
Aβ (II)	6–12	33–75	Myelinated	Sensory from skin (touch, pressure) and muscle spindle afferent
Aγ	5–8	15–40	Myelinated	Motor to muscle spindles (regulate sensitivity)
Aδ (III)	1–5	5–30	Myelinated	Sensory from skin (pain from sharp stimuli and cold)
B	< 3	3–15	Myelinated	Preganglionic autonomic fibers (to autonomic ganglia)
C (IV)	0.2–1.5	0.5–2.0	Unmyelinated	Sensory from skin (pain from dull stimuli and warmth), postganglionic autonomic fibers

Why different nerve fibers recover differently

Diameter and myelination: Larger myelinated fibers, such as Aα and Aβ, have a better recovery rate than the smaller, unmyelinated fibers, such as C fibers. This is because myelination helps protect the nerve and enhance the speed of conduction. A thicker diameter similarly aids in better conductivity. When these fibers are decompressed, they can relatively quickly regain their function.[61]

Type of function: Motor fibers (e.g., Aα) and primary sensory fibers (e.g, Aβ) might display quicker noticeable recovery after decompression because their function is more easily detectable (e.g., muscle movement and touch sensation). In contrast, the recovery of pain and temperature sensations (transmitted by Aδ and C fibers) might be more gradual or less distinct.[62]

Extent of compression: Prolonged compression can lead to Wallerian degeneration, wherein the axonal segment distal to the injury site degenerates. Recovery involves the regeneration of this axonal segment, which occurs at a rate of approximately 1 mm/day. However, while large myelinated fibers can potentially regenerate successfully, smaller unmyelinated fibers might not have the same capacity.[63]

Vascularity: Nerve fibers depend on vascularity for their nutrition. Some fibers, especially the smaller unmyelinated ones, might be more susceptible to ischemic damage during compression. Hence, their recovery after decompression might be compromised if there was substantial ischemic injury.[64]

Reinnervation potential: Even after decompression, the appropriate reinnervation of target tissues (e.g, muscles and skin) is crucial for functional recovery. While motor neurons (Aα fibers) have a specific target, the wide distribution of sensory endings (for Aβ, Aδ, and C

fibers) can sometimes lead to inaccurate reinnervation, affecting the quality of sensory recovery.[61,65]

Clinical presentation and specific nerve root tests

A typical patient with CFS presents with radiculopathy in one or both arms sometimes in combination with neck pain. There is often a component of numbness and restricted range of motion of the affected arm. The symptoms are often aggravated by neck extension, lateral flexion and rotation towards the ipsilateral side. In contrast, many patients may experience relief with shoulder abduction and neck distraction.[66]

The Spurling test (foramen compression test) is a commonly used clinical test when suspecting or investigating a patient suspected of having neurological deficits and arm pain.[67] The test is conducted by standing behind the patient and resting one hand on the patient's head (Figure 9). The physician then performs a slow extension and lateral flexion to the symptomatic side of the neck while simultaneously putting axial pressure on the head. If this aggravates the pain, the test is considered positive. The Spurling test demonstrates a specificity of 0.89 and 1.00 (with a 95% CI of 0.59–1.00) and a sensitivity of 0.38 to 0.97 (95% CI of 0.21–0.99).[68] The test also helps in differentiating between various dermatomes.[69] Consideration must also be given to the fact that there are different anatomical variations that may present with substantial dermatome overlap.[70] Testing motor strength and dermatome-bound numbness also aids in the clinical perception of which nerve roots that might be compromised.

Figure 9 Illustration of the Spurling test being performed by the examiner standing behind the subject, applying an extension, lateral flexion, and axial pressure on the subject in the foreground.

There are other clinical tests that are used on the cervical spine; for example, the neck extension test can be utilized in the clinical setting by simply extending the patient's neck backward. A positive test is the reproduction of symptoms, potentially suggesting nerve root pathology.[71]

Another useful test in assessing cervical radiculopathy is the upper limb neurodynamic Test (ULNT).[72] This test is a set of clinical tests used to assess the mechanosensitivity of the peripheral nerve tissue in the upper limb. These tests can help diagnose neural tissue dysfunction, such as nerve compression or irritation. The tests primarily involve moving the patient's arm and neck in specific ways to place stress on various nerves, thereby evaluating the nervous system's mechanical behavior.

Another clinical test for cervical radiculopathy is the Arm Squeeze Test, introduced by Gumina et al. in 2013.[73] It is a diagnostic procedure for cervical radiculopathy in which the examiner squeezes the middle third of the patient's upper arm. If the patient perceives pain radiating to a more distal part of the arm, such as the forearm or hand, the test is considered positive. There are also other tests such as the Shoulder Abduction test and the Traction-distraction test both described by Viikari-Juntura et al. [66]

A comprehensive study by Thoomes et al.[68] analyzed the efficacy of various physical tests in diagnosing cervical radiculopathy confirmed by imaging or surgery. Although many tests were assessed, few have been evaluated across multiple studies, with the Spurling test being an exception. The Spurling's test exhibited varying sensitivity but consistently high specificity.[66,74,75]

Lumbar foraminal stenosis manifests primarily as unilateral radicular pain, often accompanied by numbness, tingling, or weakness in the leg along the distribution of the compressed nerve root.[9] The sharp or burning pain typically intensifies with lumbar extension, lateral flexion, and rotation. Symptoms may be alleviated in flexed positions, offering nerve root decompression. Diagnosis is supported by imaging studies aligned with clinical symptoms.

There are a few clinical tests that can be utilized. The commonly used straight leg raising (SLR) test and the slump test are examples of tests used in the clinic in daily practice. During the SLR test the patient lies supine while the examiner lifts the patient's extended leg at the hip, keeping the knee straight. The test is positive if the patient experiences pain down the back of the leg, typically between 30 and 70 degrees of leg elevation, suggesting nerve root irritation or compression, often due to conditions such as herniated discs or degenerative foraminal stenosis.[76]

The bowstring test is a clinical examination used to detect sciatic nerve irritation or lumbar radiculopathy, particularly in cases in which standard SLR tests are inconclusive or negative.[77] The patient lies on her/his back, and the examiner raises the patient's leg to a point just before it causes pain or discomfort (as in an SLR test). Once the leg is raised, the patient's knee is slightly flexed to reduce the tension. The examiner then presses firmly with her/his fingers in the popliteal fossa, the area behind the knee. This action is akin to "stringing the bow," hence the name of the test. The test is considered positive if this compression reproduces the patient's sciatic pain or radicular symptoms that radiate along the course of the sciatic nerve.

Another clinical test is the slump test, in which the patient sits on the edge of a table, slumps forward, and extends one leg at a time while the examiner monitors for signs of pain or discomfort.[78] Positive signs, such as radiating pain or increased tension, may indicate neural tension or compression. Also, clinical examinations trying to pinpoint dermatome bound sensory disturbances and motor weakness helps in the progressing along the diagnostic path and in finding the optimal treatment. In a study comparing different lumbar neurodynamic tests the research group found that neurodynamic tests and radiculopathy assessments generally lacked diagnostic accuracy, with the slump test being the most sensitive and clinical dermatome-bound radiculopathy the most specific.[79]

Chapter 4

Imaging of the spine

The evolution of imaging modalities has profoundly impacted the accurate diagnosis and management of spinal foraminal stenosis. Historically, plain radiography was employed as the first-line imaging modality, providing an initial overview of bony structures and alignment.[80] Although beneficial, the limitation of plain films is evident in their inability to visualize nerve roots, discs, and other soft tissues directly. With the advent of computer tomography (CT) in the 1970s, detailed cross-sectional images of the spine with superior resolution of bony elements became available.[81] CT, particularly when combined with myelography (CT myelography), significantly enhanced the visualization of nerve roots and the thecal sac, making it a valuable tool for assessing foraminal stenosis.[82]

Nevertheless, the introduction of Magnetic Resonance Imaging (MRI) has revolutionized spinal imaging due to its unparalleled ability to depict soft tissues, including IVDs, nerves, and spinal cord, without ionizing radiation. MRI not only offers sagittal and axial imaging but also allows for the acquisition of images in multiple planes, granting a comprehensive understanding of foraminal stenosis in the context of associated spinal pathologies.

Today, MRI is considered the gold standard in the diagnostics of nerve root and medullar compromise in the spine.[83,84] However, in situations in which MRI is contraindicated, such as when a patient has certain metallic implants or other metal objects within their body, CT/CT myelography serves as an alternative diagnostic approach. Standard X-ray is used in the clinical setting today, but mostly for the follow-up of larger deformities, postoperative baseline images, and, in some cases, the comparison of spinal alignment between two different positions in suspected instable situations. CT is mostly used in trauma diagnostics and in pre surgical workups to better characterize osteophytes and ankylosis better. Each modality has its indications, with the choice depending on the clinical scenario, patient characteristics, and specific diagnostic requirements.

MRI sequences

MRI uses various sequences to create detailed images of structures within the body, each tailored to highlight different tissues and abnormalities.[84] In spinal imaging, specific MRI sequences are particularly useful.

T1-Weighted sequences:[85] These provide excellent anatomical detail, making them useful for evaluating the vertebral bodies and IVDs. T1-weighted images are good for assessing fat-containing structures and detecting bone marrow abnormalities.

T2-Weighted sequences:[85] These sequences are sensitive to water content and are excellent for visualizing structures with high water content, such as the cerebrospinal fluid (CSF). They are particularly useful in evaluating the spinal cord and in detecting oedema, inflammation, and various pathologies in the spinal cord and soft tissues. They can also be useful in evaluating IVDs and detecting bone marrow abnormalities especially in combination with other sequences (often T1w).

Short Tau Inversion Recovery (STIR):[85] These sequences are sometimes used in the clinic to suppress disturbing fat signals in the evaluated tissue. As such, they are more sensitive to bone marrow edema and other inflammatory changes than T2-weighted sequences.

Post-contrast T1 sequences:[85] After the administration of gadolinium-based contrast agents, these sequences are used to assess the blood-spinal cord barrier but can also supplement T1- and T2-weighted sequences in identifying areas of inflammation, infection, or tumors.

Gradient Echo (GRE) sequences:[85] These sequences are sensitive to magnetic field inhomogeneities and are particularly useful for de-

tecting hemorrhage and certain types of calcifications. They are also used for imaging ligaments and small joint structures in the spine.

Diffusion-Weighted Imaging (DWI):[86] This sequence is used to evaluate the diffusion of water molecules within tissues and can be useful in detecting spinal cord infarction. It can also be useful in detecting ischemic lesions early in the process and in characterizing lesions, for example, to differentiate between benign and malignant lesions.

Zero Echo Time (ZTE):[87] Is a technique designed to significantly reduce the echo time (TE), i.e., the time between the delivery of the radio frequency (RF) pulse and the receipt of the echo signal. Traditional MRI techniques often struggle with imaging tissues that have very short T2 relaxation times, such as bones or tissues with rapid signal decay, because the signal may decay before it can be captured at longer echo times. By minimizing the echo time to near zero, ZTE MRI allows for the capture of signals from tissues that would otherwise not be visible or be poorly represented on conventional MRI scans.

Each of these MRI sequences offers unique insights into spinal anatomy and pathology, aiding in the accurate diagnosis and management of spinal disorders. The choice of sequences and combinations depends on the clinical question at hand and the specific details needed for diagnosis or treatment planning.

MRI field strengths

Different magnetic field strengths of MRI scanners also influence the quality of the images obtained. High-field MRI systems (1.5T and 3T) deliver higher signal-to-noise ratios providing higher-resolution images than do low-field systems (0.25T – 0.6T),[88] facilitating the meticulous evaluation of foraminal stenosis.[89] However, the higher-

field-strength machines come with drawbacks such as increased purchase costs and risk of susceptibility artifacts and motion artifacts, particularly in the cervical spine where such artifacts can obscure the foramina.

MRI acquisition methodology

In MRI of the spine, the choice between acquiring volume sequences and regular stacks of images can have profound implications for image quality and diagnostic utility.[90] Volume sequences, often referred to as 3D sequences, capture the spine in a single volumetric slab, allowing post-acquisition reconstructions in any desired plane without further patient scanning. This capability is particularly beneficial in assessing complex anatomical relationships, enabling multiplanar reformatting with consistent image quality and resolution. In contrast, regular stacks of images, or 2D sequences, are acquired slice by slice in a specific plane. While they can provide high in-plane resolution, the lack of flexibility in post-acquisition plane adjustments can be limiting. Moreover, when evaluating the spine, for which both axial and sagittal views are crucial, the ability to obtain reconstructions from 3D volume sequences can be advantageous. However, the choice is nuanced: 2D sequences might offer better signal-to-noise ratios in certain scenarios and are less susceptible to specific artifacts than 3D sequences.[90] When imaging the spine, radiologists must weigh these factors in context, considering the specific diagnostic query, patient motion, and acquisition time to select the most appropriate imaging approach. Furthermore, accurate depiction of the cervical foramina demands images acquired at oblique angles, mirroring the oblique course of the foramina in this region. Obtaining oblique sagittal images at a 45-degree angle to the midline enhances the visualization of the nerve roots and intervertebral foramina, optimizing the assessment of cervical foraminal stenosis.[91]

Classification systems of foraminal stenosis

Grading instruments play a crucial role in evidence-based medicine, informing health policy and guiding the development of clinical practice guidelines.[92] They are widely utilized in creating clinical guidelines and evaluating research publications. However, their benefits can be compromised by misuse and several identified issues. A review by Irving et al. [92] has highlighted concerns with grading instruments. The authors identified the importance of validity and reliability (Figure 10), which are crucial elements of any classification system. The vulnerability to subjective interpretations, the risk of complexity, and unclear guidance are also pointed out as being important aspects to consider.

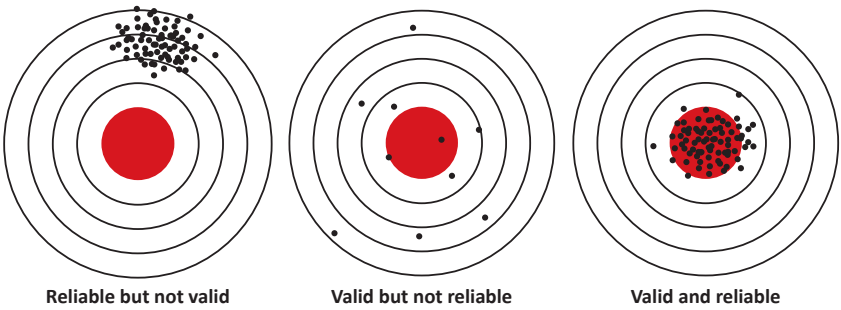

Figure 10 Illustration of the implications of validity and reliability. The bull's eye represents the true value that the test is aiming to quantify.

There are classifications for foraminal stenosis based on MRI, but their validity and correlation to symptoms has rarely been explored.[93-95]

MRI in functional positions

The concept of conducting MRI scans in functional positions is relatively nascent in the research domain, and its relevance to clinically meaningful data is still being established.[96] The terminology surrounding this subject is varied and sometimes ambiguous, potentially leading to confusion or misinterpretation as to its intent. The primary terms employed are "kinematic MRI" and "dynamic MRI," which are often used to describe this emerging technique.[97] Kinematic MRI (kMRI) and dynamic MRI (dMRI) represent distinct yet interrelated imaging modalities within the field of radiology, each with specific applications and focal points. kMRI is primarily concerned with the detailed analysis of joint kinematics, often with a particular emphasis on spinal motion. This technique is utilized to assess biomechanical changes in joints during various postures such as flexion, extension, and rotation and in weight-bearing conditions. It is especially valuable in diagnosing conditions that manifest during movement or specific postural alignments, such as spinal instability and neuroforaminal narrowing.[98]

In contrast, dynamic MRI encompasses a broader spectrum of applications, extending beyond the kinematic study of joints to include a variety of body parts and physiological functions.[99] This modality is employed not only for assessing joint and spinal dynamics but also for evaluating organ movement, cardiac function, and blood flow dynamics. It provides a comprehensive view of the body's functional anatomy under different conditions, including motion and physiological activities.

The terminology in the literature may occasionally lead to confusion, as the term "dynamic MRI" is sometimes applied to studies examining joints and bones at distinct points during movement, captured in separate images.[100] While this usage is not incorrect, employing the term "kinematic MRI" for such studies would provide greater speci-

ficity and clarity, delineating the focus on the mechanics of joint and bone movement.

While kMRI is a subset of dMRI with a specialized focus on joint kinematics, dynamic MRI represents a more inclusive category, capturing a wide range of dynamic and functional aspects of the human body. This distinction underscores the versatility of MRI technology in adapting to diverse diagnostic requirements, from detailed joint analysis to broader assessments of physiological motion and function.

MRI in functional positions in a supine position compared with an upright position

The idea of capturing images in a position in which the symptoms are usually aggravated is nothing new. Wildermuth et al. [101] explored foraminal changes in 1998 in an upright MRI, paving the way for the qualitative grading of lumbar foraminal stenosis. A fairly recent literature review called for attention to the use of upright MRI, pointing out pathologies being unmasked in the sitting position for spinal imaging.[102] The shortcoming has been the availability of upright MRI and the fact that it has lower static magnetic field strengths, usually 0.25–0.6 Tesla.[88] The downside of using an upright system is primarily the lower magnetic field strength leading to:

Reduced signal-to-noise ratio (SNR):[103] This is due to the fundamental relationship between magnetic field strength and signal generation in MRI. The strength of the magnetic field directly influences the amount of signal produced by the protons in the body. At higher field strengths, protons align more strongly with the magnetic field, resulting in greater net magnetization. When the radio frequency (RF) pulse is applied, this greater magnetization produces a stronger signal. Therefore, at lower field strengths, the net magnetization and

subsequent signals are weaker, leading to a lower SNR, which directly affects the ability to distinguish subtle differences in signal intensity between different types of tissues.

Lower resolution:[103,104] This is mainly because of the reduced SNR but also because upright systems often have less powerful gradient coils, which are essential for achieving finer spatial resolution. The weaker gradients limit the ability to create very thin slices and high spatial resolution, further affecting the overall image resolution. This can make it more challenging to detect small structures or subtle pathological changes, which is crucial when evaluating foraminal stenosis, especially in the cervical region.

Longer scan times:[103] These are due to the need to compensate for the lower SNR at lower field strengths. To improve the SNR, more signal averaging is required, which involves repeating the imaging sequence multiple times. This repetition increases the total scan time. Additionally, the longer T1 and T2 relaxation times at lower field strengths can necessitate longer repetition times (TRs) and echo times (TEs), further extending the duration of the scan. The longer scan times can be less comfortable for patients experiencing symptoms in the upright position.

Limitations of advanced imaging techniques:[104] Advanced MRI techniques and methods are being extensively explored in the search for sharper diagnostic imaging tools. These techniques often require higher field strengths to be effective, so they might not be feasible with lower-field-strength MRI systems.

A higher static magnetic field strength is obviously advantageous for examining small anatomical features such as the spinal foramina, even though there are promising ways to better develop lower field strength MRI.[105] In clinical settings, the standard supine MRI machines with 1.5 and 3 Tesla are widely utilized. Leveraging these

existing systems, while adapting to functional and symptomatic patient positions and loads using specialized devices for standard MRI scanners, offers significant advantages.

Chapter 5

Treatment strategies

Natural progression of symptoms related to foraminal stenosis

The progression rate and symptom severity vary, with some individuals maintaining a stable condition for years, while others experience rapid deterioration.[106] A vast majority of patients will experience a short-term symptomatic improvement with non-operative care.[56] Over the longer term, however, foraminal stenosis generally progresses due to the continuous wear and aging of the spinal structures.[7] Treatment approaches to foraminal stenosis are multifaceted, often starting conservatively and progressing to surgical interventions if necessary.

Non-operative management

Initial treatment usually involves conservative strategies. These encompass pain management through medications (e.g., NSAIDs and corticosteroids), physical therapy, and lifestyle modifications.[7] Therapeutic exercises aim to improve flexibility and strengthen the supporting muscles, thus alleviating pressure on the nerve roots.[107] For patients with significant inflammation, epidural steroid injections can offer temporary relief by reducing swelling and pain in the nerve roots.[108] This treatment is often more effective in the lumbar region due to accessibility.[109] There is evidence of pain relief in the short term (3–6 months) if the etiology is disc herniation, but no supporting evidence that the injections change the long-term prognosis of the symptomatic foraminal stenosis.[109,110]

Surgical interventions

When conservative measures fail or in cases of severe symptoms of foraminal stenosis in combination with radiological findings, sur-

gery may be indicated. In the cervical spine the surgical options are anterior cervical discectomy and fusion, posterior foraminotomy, or cervical disc arthroplasty.[8,111,112] In the lumbar spine, surgical options may range from a direct decompression to different foraminal relieving strategies, including decompression, indirect or direct, combined with fusion in cases in which stability is a concern.[9,113]

The treatment for spinal foraminal stenosis is highly dependent on its etiology and location, both in the cervical and lumbar spine. Understanding the underlying cause and natural progression of the condition is paramount for selecting the most effective treatment strategy. Often, a stepwise approach, transitioning from conservative management to surgical intervention, provides the best patient outcomes.

In summary, while decompression surgery can provide relief and functional restoration, the extent and speed of recovery vary based on the type of nerve fibers involved, the duration and severity of compression, and other physiological factors. After decompression, while motor functions might show rapid improvement due to the nature of the fibers and their detectable function, sensory recovery can vary, especially in terms of pain and temperature sensations. Proper post-operative care, physical therapy, and monitoring are crucial to maximizing the chances of full recovery and function restoration.[114,115]

Chapter 6

Difficulties in clinical and radiological diagnostics of symptomatic foraminal stenosis

In the endeavor of diagnosing and treating symptomatic foraminal stenosis, various classification systems are being developed. These systems ultimately aim to support decision-making through algorithms that guide patient referrals and the selection of treatment methods. While these classification systems are gradually being validated, there is no widespread acceptance of what systems to use and no guidance on how to use them in clinical practice.

Second, the standard radiological investigation for both cervical and lumbar foraminal stenosis is an MRI investigation in a supine relaxed position, while many patients describe the distinct aggravation of symptoms in particular functional positions. These positions are usually when the spine is extended and, in the neck, especially when it is laterally bent and/or rotated. These patients sometimes present with more than one suspected foraminal stenosis without clear clinical correlation, raising the question of which foramina is responsible for the symptoms. There have been studies demonstrating that compression in the lumbar spine during MR image acquisition can reveal pathology not seen in a standard supine relaxed setting.[116,117] MRI in an upright position has also been tested demonstrating significant changes to different intervertebral properties and thereby revealing information not seen in a supine position.[97,118] Furthermore, it has been shown that cervical foraminal changes can be detected with MRI when comparing images taken in different positions of the neck.[98,119] Prior work is suggesting that imaging of the spine in different positions may reveal clinically important information aiding in decision-making regarding different treatment options. The data are limited and, to our knowledge, no available device is available to control the cervical spine during MRI acquisition. If the spine could be examined in positions in which the patient experiences symptoms, this might aid in the diagnosis of patients with more than one suspected foraminal stenosis. Furthermore, while prior research has explored cervical spine biodynamics[20, 31, 35], there remains a notable paucity in the literature concerning the biodynamics of the cervical spine in patients experiencing intermittent arm radiculopathy due to foraminal stenosis.

Chapter 7

Aim

The overall aim of the thesis is to explore changes in spinal foraminal properties and the surrounding tissues with MRI conducted during applied forces.

The specific aims of the separate studies were as follows:

Study I
To systematically review and report on validated classification systems for the assessment of cervical and lumbar foraminal stenosis.

Study II
To study possible changes in foraminal properties in the lumbar spine during axial loading, using both quantitative and qualitative measures in patients with LBP but without spinal nerve root symptoms.

Study III
To evaluate the practical use of a newly designed cervical compression device, establish a protocol for its usage, guarantee the capture of clinically satisfactory MR images while employing the device, and investigate any potential changes of the foramina in a cohort of healthy controls.

Study IV
To examine patients with intermittent arm radiculopathy with MRI during a simulated Spurling test, investigate the tolerance of the provocation, and, furthermore, study possible changes in foraminal properties comparing unprovoked and provoked MR images.

Study V
To analyze intervertebral motions occurring during the Spurling test by employing zero-echo-time (ZTE) MR images and the Sectra® CT-based Micromotion Analysis (CTMA) software in patients with intermittent arm radiculopathy.

Chapter 8

Methods

Study inclusion criteria and patient selection

Study I

This systematic review was performed in adherence to PRISMA guidelines. Electronic searches were performed by a professional librarian in the Cochrane, Embase, Medline, and PubMed databases, encompassing 30 years of literature in English up to September 2021. The search strategy encompassed three categories—i.e., foraminal stenosis, MRI, and scoring— utilizing various terms in each category to capture all relevant nuances and synonyms. Inclusion required at least one term from each category. The initial category included terms such as foraminal stenosis and neuroforaminal stenosis, the second MRI-related terms, and the third involved scaling, grading, and classification terms. From 823 identified articles, two authors reviewed and excluded case reports, descriptive papers, and those focusing solely on radiographic techniques. Further exclusions were articles with unclear grading systems, lacking reliability data, or using ad hoc classifications. This process narrowed the selection to 61 full-text articles, with 14 ultimately meeting all predefined reliability evaluation criteria for inclusion in the review.

Study II

Patients were consecutively recruited as a sub-cohort for a study examining lumbar spinal loading effects on various spinal structures in individuals with chronic non-specific LBP, using MR images both with and without spinal loading. Inclusion criteria in this study encompassed an age range of 20–70 years and a history of chronic non-specific LBP lasting at least three months. Exclusion criteria included the presence of sciatica symptoms, claustrophobia, prior back surgery, clinical indications of nerve root affliction, or the absence of adequate sagittal MR images both with and without axial spinal

loading. Eighty-nine patients met these criteria, with an average age of 43 years (27–66 years), comprising 33 women and 56 men.

Study III

Between November and December 2020, at Sahlgrenska University Hospital in Gothenburg, Sweden, MRI was performed on ten healthy subjects. These subjects, recruited from the hospital staff, had no history of arm radiculopathy or past cervical surgeries, although previous instances of unexplained neck pain were deemed acceptable for inclusion in the study. The study subjects comprised four females and six males, 27–55 years old.

Study IV

Between March and May 2022, ten patients with suspected cervical foraminal stenosis referred to our spine surgery unit were invited to participate. Criteria for inclusion were intermittent arm radiculopathy, a positive Spurling test, age of 20–60 years, and recent MRI results showing one or two stenotic cervical foramina.

Study V

The patients in this study were the same cohort included in Study IV.

Ethical considerations

All studies were conducted in accordance with the Declaration of Helsinki and received approval from the Regional Ethical Review Board in Gothenburg, Sweden (Study II, Dnr [483–17]; studies III-V,

Dnr [574–18]). All participants received oral and written information about the study in which they were invited to participate, and all provided their written informed consent.

The compression devices

The lumbar compression device (Study II)

All patients underwent lumbar spine MRI examinations using a 3T scanner. The MRI sequences were initially performed in a relaxed position and then under axial loading, with a 50% body weight load applied using a Dynawell® (Dynawell Diagnostics Inc., Henderson, NV 89052, USA) compression device, with both sequences using identical scan parameters (Figure 11). The axial loading simulated by the device mimicked the anticipated stress on the lumbar spine experienced in an upright position.

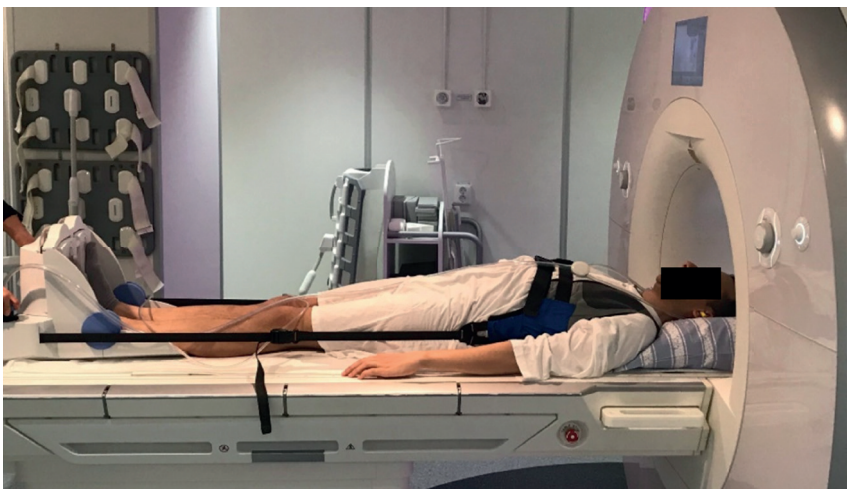

Figure 11 The Dynawell® compression device strapped on a patient about to enter the MRI gantry. The image is from Figure 2 in the article "Axial Loading during MRI Induces Lumbar Foraminal Area Changes and Has the Potential to Improve Diagnostics of Nerve Root Compromise," by Hebelka, H., Rydberg, N., Hutchins, J., Lagerstrand, K. & Brisby, H. J, published by MDPI in J Clin Med 11. 2022 April 11;11(8);2122. Licensed under CC BY.

The Dynamic MRI Compression System – DMRICS (Studies III–V)

Our research group developed an MRI-compatible compression device, the Dynamic MRI Compression System (DMRICS, with pending Patent no 2251201–6) see Figure 12, capable of applying monitored forces through a water hydraulic system. This device, which facilitates individual application of force, controls sagittal extension, flexion, lateral flexion, slight rotation, and axial compression during MRI sessions, with subjects in a supine position. Users wear a helmet, connected by long hoses to the water hydraulic system, and rest their feet on an adjustable footplate, accommodating various body lengths up to 2000 mm, with BMI restrictions untested but presumed accommodating unless limited by MRI gantry size. The system's control board (Figure 13), located in the MRI control room due to its incompatibility with the MRI, induces forces via linear actuators, applying them in 1-mm increments while monitoring to ensure slow, measured movements. The data are recorded using our custom software, DMRICS 1.0. The patient-positioning component of the device weighs approximately 9 kg and is designed to minimize discomfort and prevent distortions during use, avoiding the use of hard materials in direct contact with the user.

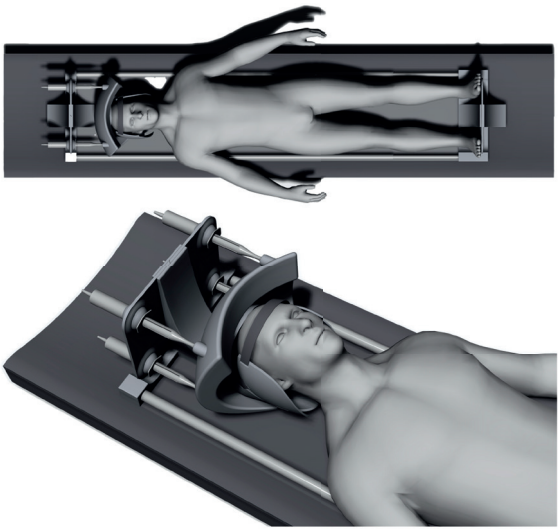

Figure 12 The top illustration of the DMRICS from a coronary view of the part that goes into the MRI gantry with the patient ready for an MRI scan. The lower illustration shows a closer view of the cranial part where the head is strapped into the helmet, which in turn is connected to four hydraulic cylinders.

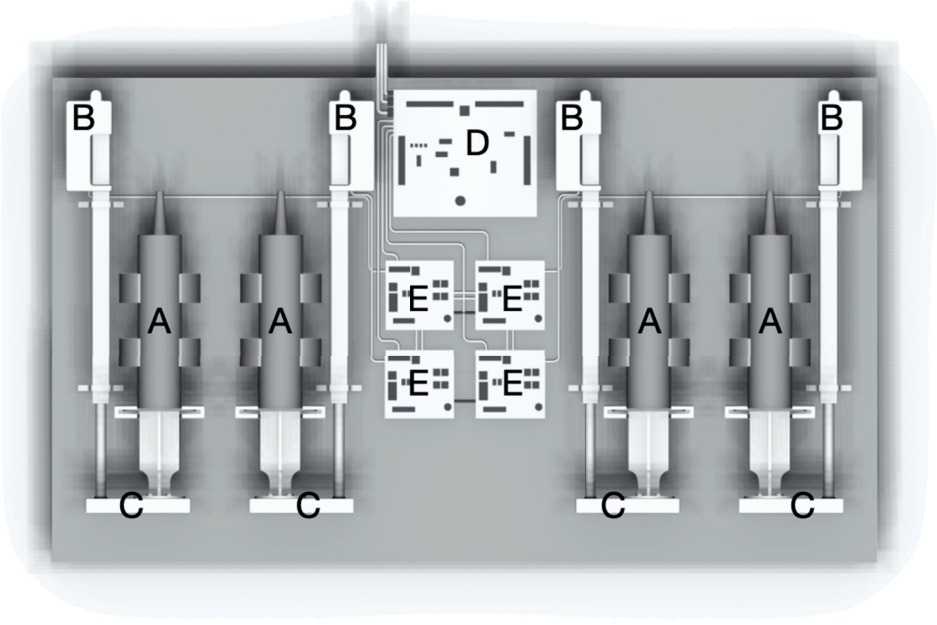

Figure 13 Schematic of the control board showing the principals of operation: the dark grey cylinders (A) are connected to water-filled hoses that are connected to the corresponding cylinders on the helmet. The base of each cylinder is connected to a linear actuator (B) via a force measuring (C) equipment. A Linux-based motherboard (D) is connected to individual motor controllers (E).

Methods of imaging and scanning areas/structures

Study I

In this systematic review, one inclusion criterion was that the classification system needed to be based on MRI, but not on any specific sequence.

Study II

All patients underwent an MRI of the lumbar spine (L3/S1) using a GE 3T Signa scanner (GE Healthcare, Chicago, IL, USA), both without and with axial loading, maintaining the same scan settings. The MRI included sagittal T1-weighted sequences (TR 573 ms, TE 7.7 ms, slice thickness 3.5 mm) and sagittal T2-weighted sequences (TR 3993 ms, TE 107.6 ms, slice thickness 3.5 mm).

Study III

MRI was conducted using a GE 3T scanner (Architect Medical Systems Waukesha, WI, USA), software version DV.29. The imaging protocol included a three-dimensional T2-weighted fast spin echo sequence with a slice thickness of 1 mm and a field of view (FOV) measuring 25 x 25 cm, utilizing an air coil for enhanced signal reception. Subjects were initially imaged in a relaxed position, followed by a provoked position to mimic a Spurling test (i.e., head extended, laterally deviated, and slightly rotated). Adjustments in force were made via the control board. The 3D volume sequences could subsequently be adjusted for accurate neuroforamen imaging at a 45-degree angle. The C4–C7 foramina were scanned on the right side. Additionally, sagittal images were taken to evaluate cervical

lordosis. MR images were anonymized and checked for quality before analysis.

Studies IV and V

Using a GE 3T MRI scanner with an air coil, T2-weighted images were obtained in the oblique sagittal plane (TR 3910 ms, TE 102 ms, FOV 27 x 27 cm^2, matrix 280 x 280, voxel size 1 mm^3) and in the axial plane (TR 1292 ms, TE 90.85 ms, FOV 26 x 26 cm^2, matrix 400 x 280, voxel size 0.6 x 0.9 x 5 mm) using GE Software SW 29.1.

MRI was conducted in a relaxed supine position and then during a simulated Spurling test. The Spurling position was reached by slowly adding forces moving the patient's head and neck into the position. The application of force ceased once the patient indicated the onset of either arm pain or unbearable discomfort, ensuring that she/he could still endure a 3-minute scan. Multiplanar reconstruction made it possible to fine tune post scanning. Standard image storage protocols were used.

ZTE images were also captured in both unprovoked and provoked states for Study V. The following ZTE imaging parameters were utilized: repetition time (TR) was calibrated to 366.38 milliseconds, echo time (TE) was minimized to an ultra-short duration of 0.02 milliseconds, and the selected slice thickness (ST) was 1.2 millimeters, the FOV was 25 x 25 cm, and the images were acquired with a matrix resolution of 1.2 x 1.2 x 1.2 mm. These images were adjusted to match CT image intensity and modified in their DICOM attributes for CTMA software analysis, enabling micromotion assessment.

Measurement and observers

Study I

The 14 included studies were analyzed in detail by two of the authors. Key elements were compiled into a table including descriptions of the studies, as well as their statistics, validation, and conclusions.

Study II

Measurements focused on the intervertebral foramina, with evaluations carried out on levels L3/L4–L5/S1. Using AGFA HealthCare software, 534 foramina across these spinal levels were measured on sagittal T2-weighted sequences, choosing the smallest foraminal area in the images (Figure 14). The smallest areas were measured, and foramina appearing in multiple image slices were assessed from the image showing the least area. Qualitative assessments were made on T1w sequences according to the Lee et al.[120] classification system for foraminal stenosis (Figure 15) and the Pfirrmann grading system for disc degeneration.[121] The evaluations were conducted blindly by a radiology resident who had undergone supervised training, with repeated measurements performed for reliability and validation. All initial measurements were made on images without loading. The images taken with the axial load where evaluated a month later, without reference to the initial data.

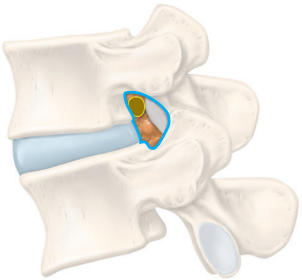

Figure 14 Illustration of the outlined foraminal area in the lumbar spine.

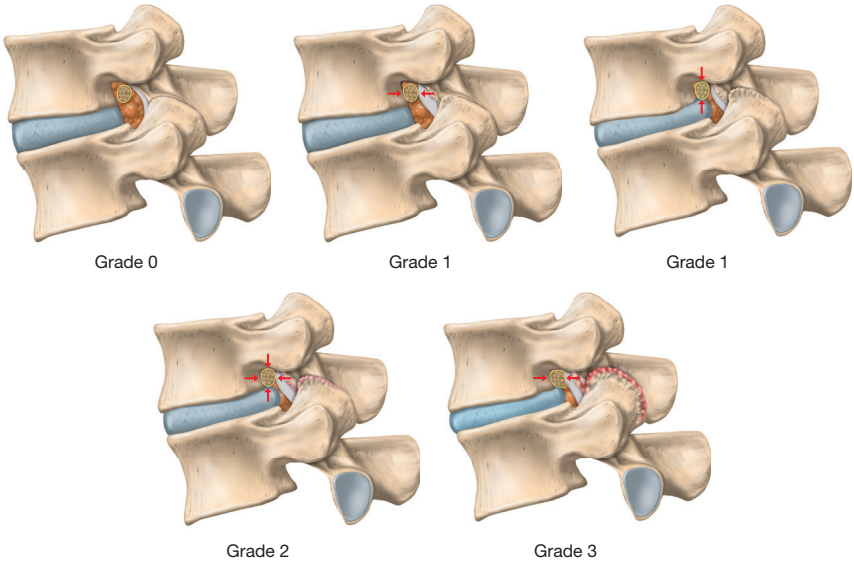

Figure 15 An illustration of the Lee classification system. Grade 0 indicates absence of stenosis and intact perineural fat. Grade 1 is characterized by either transverse or vertical foraminal narrowing accompanied by loss of perineural fat. Grade 2 is identified by complete loss of perineural fat and foraminal constriction without affecting the nerve root's shape. Grade 3 is marked by complete perineural fat obliteration and obvious morphological deformation of the nerve root.

Study III

Three quantitative measurements and two qualitative classifications were utilized on images taken in both the relaxed and provoked conditions. The studied levels were on the right side between levels C4 and C7. The quantitative measures were the lordosis angle between C3 and C7, foraminal area on oblique sagittal images, and foraminal cross-distance on axial images (Figure 16). The baseline foraminal compromise was also assessed using the Park[94] and Kim[95] classification systems. The RadiAnt DICOM Viewer 64-bit (2021.1–17805) was utilized for these measurements and gradings after observers were trained on the software. Images in both the relaxed and compressed states were anonymized for unbiased observation. Baseline disc de-

generation was graded using the Pfirrmann classification system.[121] All readings were measured by one radiologist and then reevaluated after a four-month period to determine intrarater reliability, while a second radiologist measured a subset for interrater reliability.

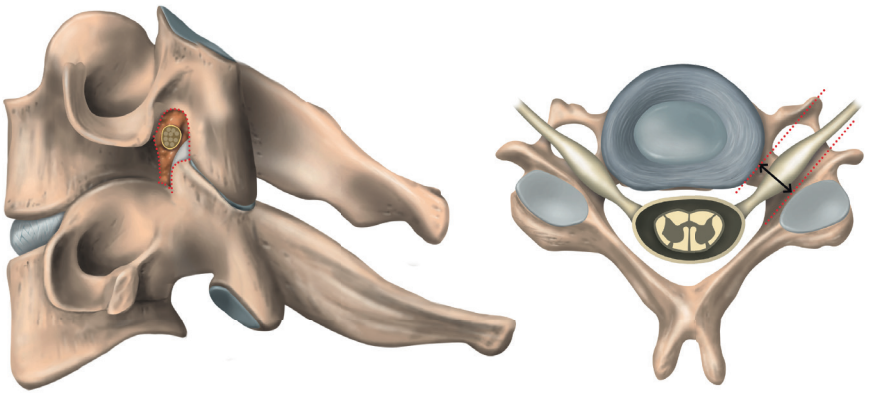

Figure 16 To the left, the foraminal area is outlined on the oblique image plane and to the right, the foraminal cross-distance is shown on the axial image plane.

Study IV

An experienced radiologist evaluated the foramina between the C4 and C7 vertebrae, examining the symptomatic side in both the relaxed position and the simulated Spurling position. All images were coded to blind the observer as to patient identities to preclude bias. The foraminal area on the oblique images and the foraminal cross-distance on the axial images were measured as in the prior study. For classification of the foraminal stenosis, the radiologist used the validated grading systems of Park[94] and Kim[95] and graded images taken in both the relaxed and provoked positions (Figures 17 and 18). The Pfirrmann grading system[121] was used to determine the level of disc degeneration. All patients filled out the Neck Disability Index (NDI) and EQ-5D

5L instruments before the examination. Agfa Enterprise Imaging software was the standard tool for all measurements and classifications. The reliability of these measurements with the DMRICS was verified in Study III, which showed an excellent intrarater reliability (>0.98) and a good level of interrater reliability (>0.62). After the procedure, the patients reported whether the provocation induced concordant arm pain.

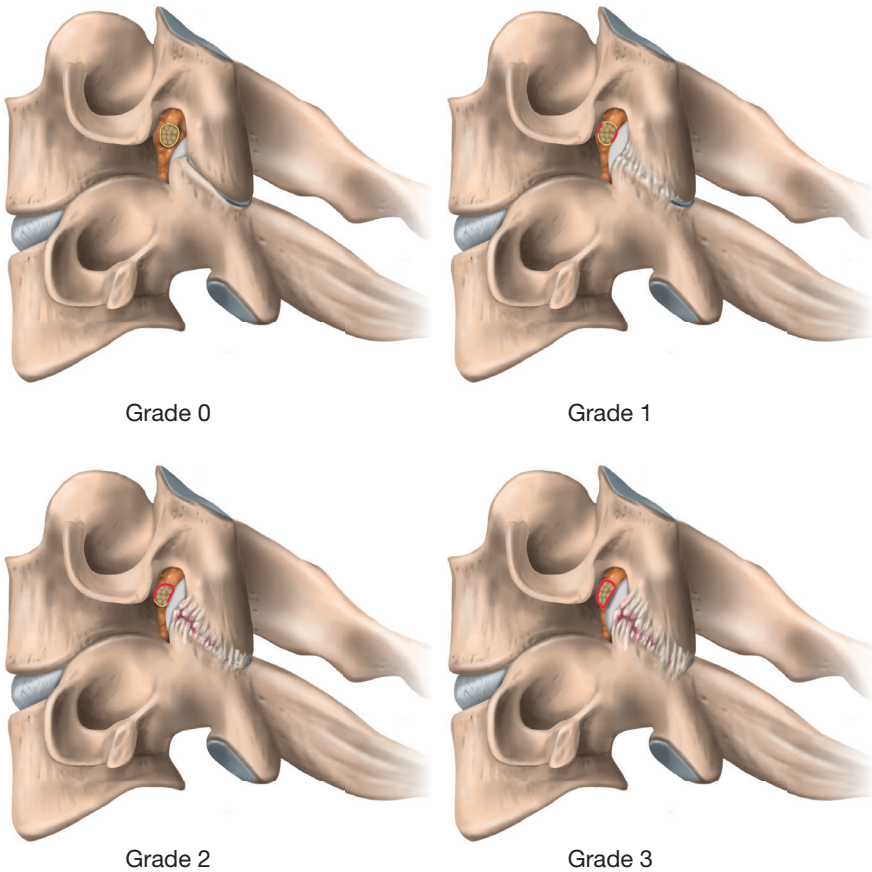

Figure 17 The Park system for classifying cervical foraminal stenosis from oblique sagittal MRI is outlined as follows: Grade 0 indicates no signs of stenosis or loss of perineural fat. Grade 1 shows less than 50% obliteration of perineural fat. Grade 2 is characterized by more than 50% obliteration of perineural fat. Lastly, Grade 3 presents with a nerve root that has collapsed morphologically.

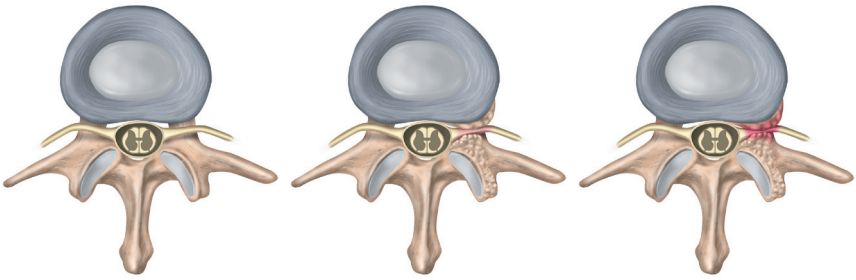

Figure 18 A diagrammatic representation of the Kim grading scale. The first images to the left illustrate a Grade 0 condition, indicating that the narrowest part of the neural foramen is wider than the extraforaminal part of the nerve root. Grade 1 is characterized by neuroforaminal stenosis in which the narrowing is less than 50% relative to the extraforaminal part of the nerve root. Furthermore, Grade 2 is characterized by a reduction in width greater than 50% compared with the extraforaminal part of the nerve root.

Study V

The ZTE MRI scans yielded CT-like images, which were imported into the Sectra® CTMA software (Sectra AB, Teknikringen 20, 583 30 Linköping, Sweden). This application constructed a three-dimensional model of the cervical spine on the symptomatic side of the C4–C7 segments. A CTMA researcher aligned the images from the patient's neutral stance with those from the simulated Spurling test, fine-tuning the alignment manually as per CTMA protocols.[122-124]

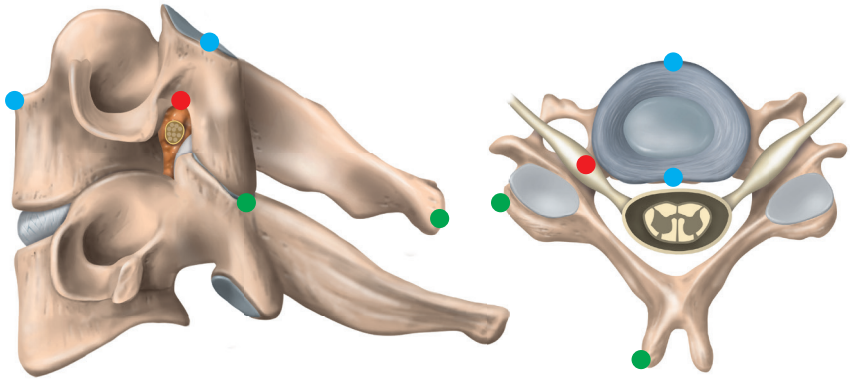

Figure 19 Illustration of the chosen points of interest.

The software then assessed the movement between adjacent vertebrae (C4/C5, C5/C6, C6/C7, and C3/C7) by comparing their positions in the relaxed and Spurling test images. It calculated the linear and angular movements across the sagittal, coronal, and axial planes. Reference points were five key locations on each vertebra (Figure 19): the foramen's peak from an oblique perspective, the facet joint's lowest point, the spinous process's rear tip, and the upper posterior and anterior corners of the vertebra as seen from the side.

Statistical analysis

Study I

All included studies were required to report on intraclass correlation coefficient (ICC) statistics to gauge the reliability of the classification system in question.

Study II

Measurements of the foramina were compared with and without load using paired *t*-tests, with a significance threshold of $p < 0.05$. To gauge consistency within and between observers, the ICC was computed, and the results were interpreted using Cicchetti's criteria: scores <0.40 signify poor consistency, 0.40–0.59 moderate consistency, 0.60–0.74 good consistency, and 0.75–1.00 excellent consistency. For categorical data, Cohen's kappa statistic was applied, with values over 0.75 indicating significant agreement. SPSS version 27.0 (IBM, Armonk, NY, USA) was utilized for all statistical evaluations.

Study III

The quantitative data gathered did not follow a normal distribution, so the Wilcoxon signed-rank test was employed to identify any significant variations in the continuous variables. The consistency of measurements made by the same observer (intraobserver consistency) and by different observers (interobserver consistency) was measured using ICC statistics. ICC scores <0.5 signify low reliability, 0.5–0.75 moderate reliability, 0.75–0.90 good reliability, and >0.90 excellent reliability. IBM SPSS version 28 was utilized to carry out the statistical analysis.

Study IV

To assess differences between groups, the Mann–Whitney U-test was applied. For within-group comparisons, the Wilcoxon matched-pairs signed-rank test was utilized. The Spearman rank correlation coefficient was employed to evaluate the relationship between quantitative and qualitative variables, as delineated by Park[94] and Kim.[95] We calculated ordinal logistic regressions to gauge the magnitude of the differences in qualitative variables between groups and presented the results as odds ratios with 95% confidence intervals. A 5% significance threshold was adopted. Interpretation of the NDI followed Vernon et al.[125] guidelines: scores of 0–4 imply no disability, 5–14 a mild disability, 15–24 a moderate disability, 25–34 a severe disability, and >35 a complete disability. Statistical analyses were conducted with SPSS software version 28 and Stata version 17.0.

Study V

To present the demographic data of the participants, descriptive statistical methods were employed. Statistical comparisons were con-

ducted using two distinct approaches: mixed models, which utilized the full range of measurements, and a non-parametric method, which relied on the mean change per level. The mixed models approach took into account multiple data points per vertebra within an individual, whereas the non-parametric method applied the Wilcoxon Signed Rank test to evaluate the mean differences between the non-suspected and the suspected stenotic levels for each individual. The diagnostic plots for the mixed models were evaluated and deemed adequate. An unstructured covariance pattern was assumed, with separate estimations for the non-suspected and pathological levels. All the statistical tests applied were two tailed, with a *p*-value under 0.05 being indicative of statistical significance.

Chapter 9

Results

Study I

Cervical spine

In the cervical spine, two validated MRI-based classification systems for foraminal stenosis were identified. The Park system,[126] which employs oblique sagittal planes and the Kim system[95] using axial image planes. Direct comparisons between these systems indicated that both exhibit strong interobserver reliability and agreement.[127] Notably, the Park system tends to assign higher grading scores, yet these grades are marked by heightened reliability. Additionally, a modified version of the Kim system has been proposed, intended to enhance correlation with clinical symptoms, with supportive data presented.[128] All three systems, i.e., the Park, Kim, and the modified Kim systems, were evaluated in a study by Lee et al.,[129] who confirmed their good interobserver reliability. The Park and the modified Kim systems both displayed a relatively high correlation with clinical manifestations, whereas the original Kim system demonstrated a moderate correlation. Kintzele et al.[91] validated the Park system's strong interobserver reliability and noted that traditional non-oblique sagittal images might underestimate foraminal gradings. Several studies have affirmed the good interobserver reliability of both the Kim and Park systems, with two studies also linking them to clinical manifestations.[108,130,131] These studies highlighted that the Park system could effectively predict positive neurological manifestations at higher gradings. Figure 20 demonstrates the relationships between the classifications and the research groups that have validated them.

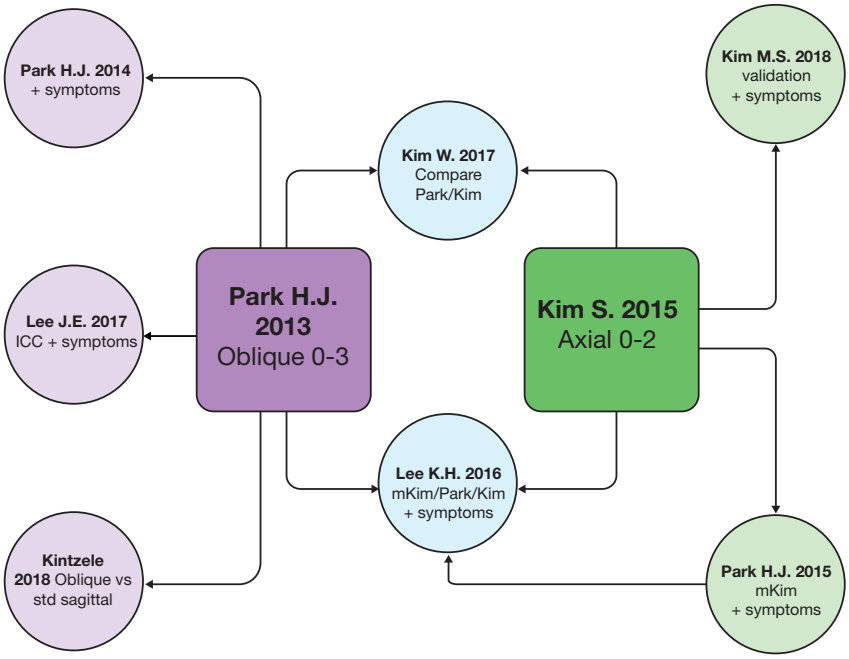

Figure 20 A mind map of the connections of validation research done of the classification systems of cervical foraminal stenosis.

Lumbar spine

For the lumbar spine, only one validated classification system was identified, developed, and presented by Lee et al.[93] in 2010. This system relies on the assessment of MRI images of the sagittal plane. It later gained validation showing moderate interobserver reliability and a strong correlation with clinical manifestations.[132] Additionally, Kang et al.[133] further validated the Lee system, demonstrating good interobserver agreement. Notably, in a surgical patient group, the Lee system's grading for the L5/S1 region displayed a lower interobserver agreement.[134] Hofmann et al.[135] reported moderate to strong

kappa agreement across observers of varying experience levels, from students to spine surgeons, underscoring the importance of comprehensive instructions for reliable grading. Figure 21 offers a comprehensive overview of the classification system and the validation done. An early concept of the qualitative approach to lumbar foraminal stenosis classification proposed by Wildermuth et al.[101] influenced the development of the Lee system. Although the Wildermuth classification, which employed CT imaging, was not initially identified in the review due to the search criteria, it is included in the discussion and depicted in the illustration.

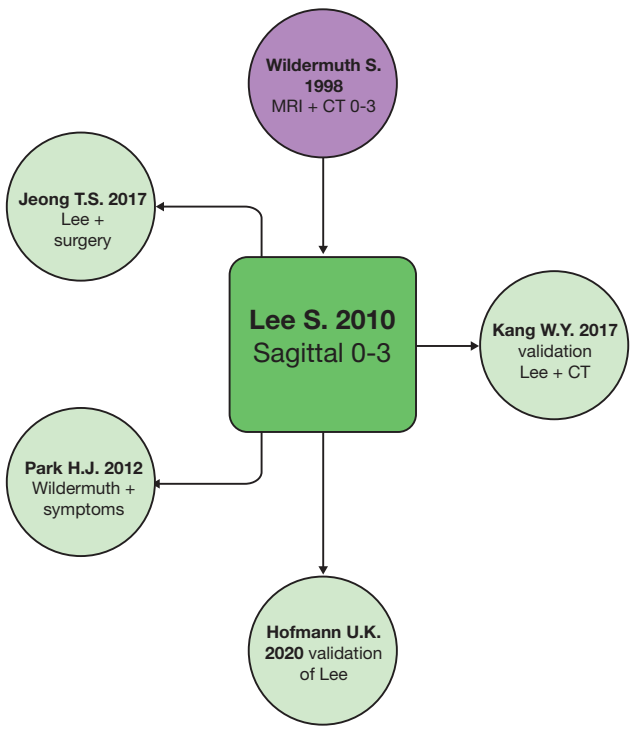

Figure 21 A mind map of validation research related to the Lee classification of lumbar foraminal stenosis.

Study II

Study cohort and baseline data: A total of 98 patients were consecutively included at the first stage. After applying the exclusion criteria, 89 were enrolled (33 women and 56 men), with a mean age of 43 years (range 27–66 years). A total of 267 discs levels and 534 foramina were evaluated. The Pfirrmann gradings of the discs were distributed as follows: Grade 2 (n = 67), Grade 3 (n = 89), Grade 4 (n = 87), and Grade 5 (n = 24).

Foraminal Area Measurements: The study observed a mean reduction of 2.2% in foraminal area (from 0.89 cm^2 to 0.87 cm^2, p = 0.002) when comparing MRIs without and with spinal loading; see Figure 22 for an example of the outlined foraminal area.

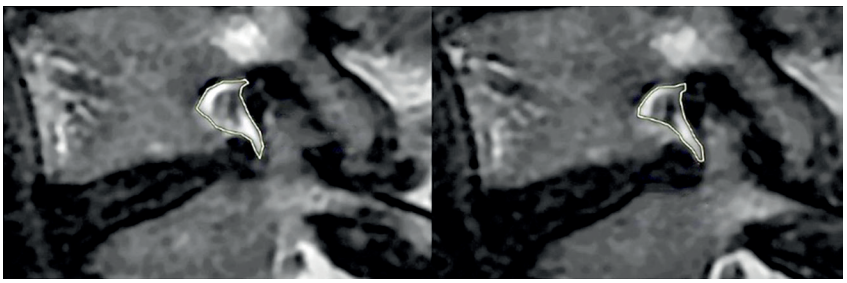

Figure 22 MRI of the right L4-L5 foramina without spinal loading alongside an MRI of the same foramina under axial loading. The area for measurement is highlighted in both images, and a decrease in the measured area is noted. Additionally, the MRI with loading shows a discernible decrease in the fat surrounding the nerve root. Figure 2 from "Axial Loading during MRI Induces Lumbar Foraminal Area Changes and Has the Potential to Improve Diagnostics of Nerve Root Compromise", by Hebelka, H., Rydberg, N., Hutchins, J., Lagerstrand, K. & Brisby, H. J, published by MDPI in in J Clin Med. 2022 Apr 11;11(8):2122. Licensed under CC BY.

The changes varied, with some foramina increasing by up to 58% and others decreasing by 42%. At specific lumbar levels (L3/L4 and L4/L5), a mean area reduction was noted during loading, but no significant change was observed for L5/S1. The distribution of these changes and the comparison of foraminal areas with and without axial spinal loading across all levels are summarized in Table 5.

Table 5 Showing the foraminal area with and without axial loading and the difference between the two, including statistical significance level. * The values are presented as mean plus standard deviation (SD).

Levels	Without Axial Load (cm^2)*	With Axial Load (cm^2)*	Paired Differences (cm^2)*	*p*-Value
All foramina n = 534	0.89 (0.27)	0.87 (0.26)	−0.02 (0.15)	0.002
L3/L4	0.99 (0.29)	0.96 (0.28)	−0.03 (0.17)	0.036
L4/L5	0.80 (0.20)	0.78 (0.20)	−0.03 (0.11)	0.004
L5/S1	0.87 (0.27)	0.86 (0.25)	−0.008 (0.15)	0.47

Qualitative Foraminal Evaluation: According to the Lee classification system, most foramina were graded as 0, indicating no stenosis. Upon loading, 25% of the foramina changed grade, with 19% showing a higher grading (indicative of narrower foramina). Among foramina that decreased in area, 22% were evaluated as having a higher grade and 72% as remaining at the same grade.

Reliability Measures: The ICC between different observers was 0.76 (95% CI: 0.62–0.85), while the intra-observer ICC was 0.96 (95% CI: 0.93–0.97), both indicating excellent reliability.

Study III

Study cohort and baseline data: The study included ten healthy volunteers, six males and four females, aged 27–55 years. Examination of the C4–C7 disc levels revealed moderate degeneration across the cohort, with Pfirrmann grades between 3 and 4 for most evaluated discs. Foraminal stenosis was mostly absent or mild among the participants, with 26 out of 30 foramina receiving a Park grade of 0 or 1 on oblique MRI, and 25 out of 30 receiving a Kim grade of 0 or 1 on MRI without axial load.

The DMRICS and image quality: The novel compression device demonstrated good usability. All participants could comfortably use the device without any reported discomfort or claustrophobia. The device functioned reliably and predictably throughout the study, and the application of relative force was visually traceable. The MRI acquisition time was brief, at approximately three minutes per volume sequence, culminating in a total examination period of roughly six minutes for both the relaxed and compressed positions. Image quality was consistently of clinical grade quality (Figure 23), save for one instance of potential motion-induced artifact over one foramina during a compressed-state scan, which was subsequently omitted from analysis.

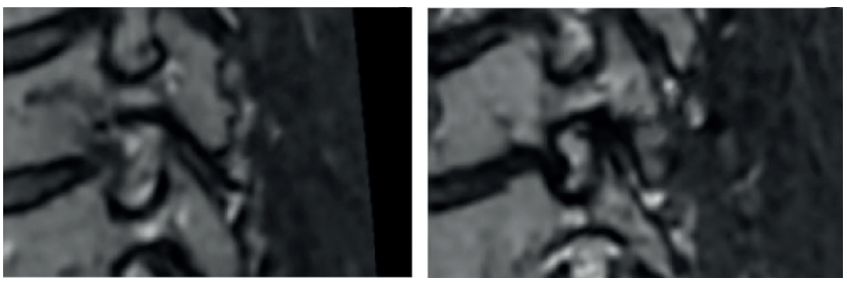

Figure 23 To the left C4/C5 foramina in a relaxed state. To the right, the same patient and level but during a simulated Spurling test.

Quantitative foraminal findings: The simulated Spurling test led to a significant increase in cervical lordosis, averaging 9.4 degrees (p =0.013), see Table 6. A notable mean reduction of 32% (p <0.001) in foraminal cross-distance was observed post-compression. Although the mean foraminal area on oblique semi-sagittal images did not exhibit a statistically significant change, individual responses varied: 15 foramina showed an increase in area, while 14 showed a decrease. This suggests a differential impact of compression across various foramina within the same individual.

Table 6 Quantitative data on measured differences between relaxed and simulated Spurling test.

	Level	Mean		Difference		P	Confidence Interval	
	Disc	UC*	C**	Mean	%	*P*-value	Lower	Upper
Cervical angle ° (SD)	C3/C7	12.290 (9.600)	21.690 (8.020)	9.400	176	0.013	3.770	15.029
Sagittal area cm^2 (SD)	C4/C7	0.277 (0.104)	0.259 (0.131)	0.018	−6	0.581	−0.049	0.013
Axial distance mm (SD)	C4/C7	2.590 (0.993)	1.749 (0.573)	0.841	−32	< 0.001	−1.189	−0.494

*Uncompressed. **Compressed

Reliability measures for the acquired quantitative data revealed excellent intraobserver agreement and good interobserver agreement, as detailed in Table 7.

Table 7 Intra- and interobserver agreement. Observers A and B. [a]Intraclass Correlation Coefficient. [b]Weighted Kappa. [c]Scale 0–5. [d]Scale 0–3. [e]Scale 0–2.

Measure	A vs A	A vs B
ICC[a]		
Cervical angle	0.987	0.867
Sagittal area	0.991	0.652
Axial distance	0.981	0.616
K[b]		
Pfirrmann[c]	0.96	0.265
Park[d]	0.935	0.409
Kim[e]	0.977	0.461

Study IV

Study cohort and baseline data: The inclusion resulted in ten patients with intermittent arm radiculopathy and MRI-verified foraminal stenosis on one or two levels, translating to the examination of 30 foramina. Baseline data reflected an average age of 44.5 years (range 29–51 years), with NRS neck and arm pain rated at 4.6 (SD 1.84) and 5.2 (SD 2.95), respectively. The mean EQ-5D 5L was 0.6 (SD 0.18) and the NDI was 26.6 (SD 10.3). The Pfirrmann classification predominantly identified grades 3 and 4, with half of the cases displaying moderate disc degeneration.

Patient experience and image quality: All subjects were comfortably positioned within the DMRICS both outside and inside the MRI scanner. The clinical image quality was satisfactory in nine out of ten cases (Figure 24).

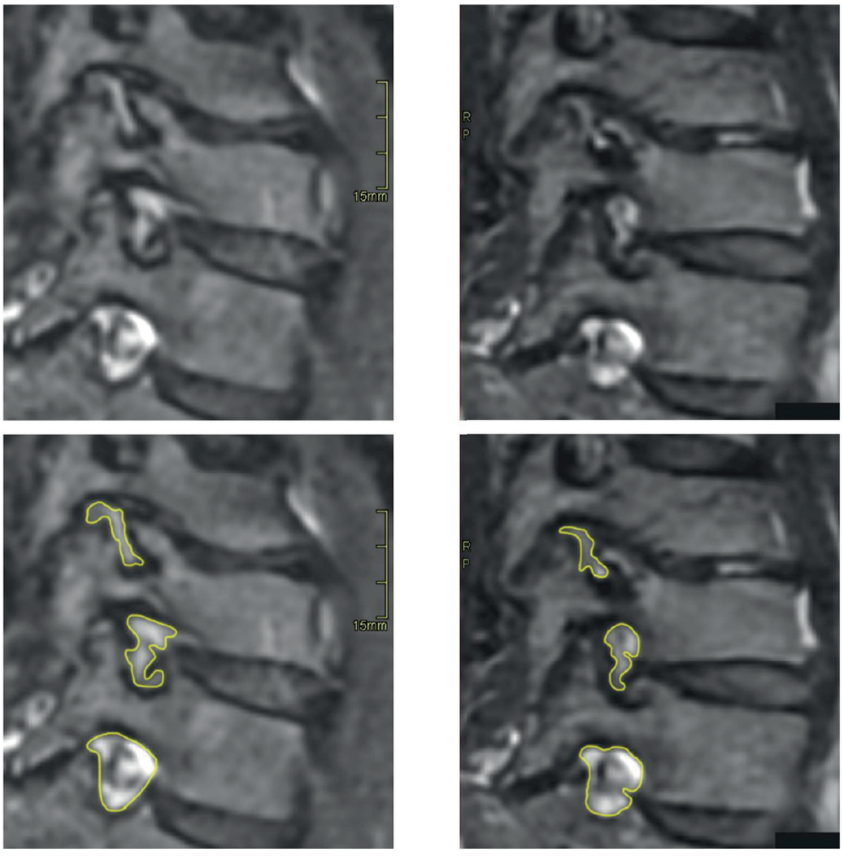

Figure 24 The left images present one patient in the relaxed state, while the right images were captured during the Spurling test of the same patient. The demarcated foraminal area is indicated in the images below. *Figure 2 from "Cervical Foraminal Changes in Patients with Intermittent Arm Radiculopathy Studied with a New MRI-Compatible Compression Device,"* by Hutchins J et al., published by MDPI in J Clin Med. 2023 Oct 12;12(20):6493. Licensed under CC *BY.*

Force Application via DMRICS: In the majority of cases (seven out of nine), the force exerted was increased by at least 50% on the symptomatic-side posterior cylinder when contrasted with the opposite side anterior cylinder, to replicate a Spurling test. Please find further technical description section 8: "Methods."[136]

Modifications in pain scores and concordance with typical symptoms: Upon administering the simulated Spurling test, we observed a rise in the neck NRS from an initial average of 4.6 (SD 1.84) to 6.8 (SD 2.25, *p*-value: 0.011). Similarly, the arm pain NRS increased from 5.2 (SD 2.94) to 6.7 (SD 3.09, *p*-value: 0.017). Notably, nine out of ten of the participants recognized that the arm pain induced by the force exerted through the DMRICS was concordant with their intermittent arm pain.

Qualitative gradings during a Spurling test: Provocation resulted in notable shifts in the Park[94] and Kim[95] classification gradings, with both showing a statistically significant difference ($p = 0.000$). Following the simulated Spurling test, all foramina previously identified as stenotic were categorized as at least Park grade 2 or 3. Changes varied, with some classifications increasing by one grade, while others increased by two. Out of 27 assessments, Park gradings rose in 13 instances, and Kim gradings in nine following provocation. Nonetheless, these grading escalations did not correspond to significant changes in the quantitative measurements. Foramina that were initially rated as Park grade 2 or 3 exhibited only slight variations in size, indicating reduced dynamism in segments with advanced degeneration, as illustrated in Figure 25.

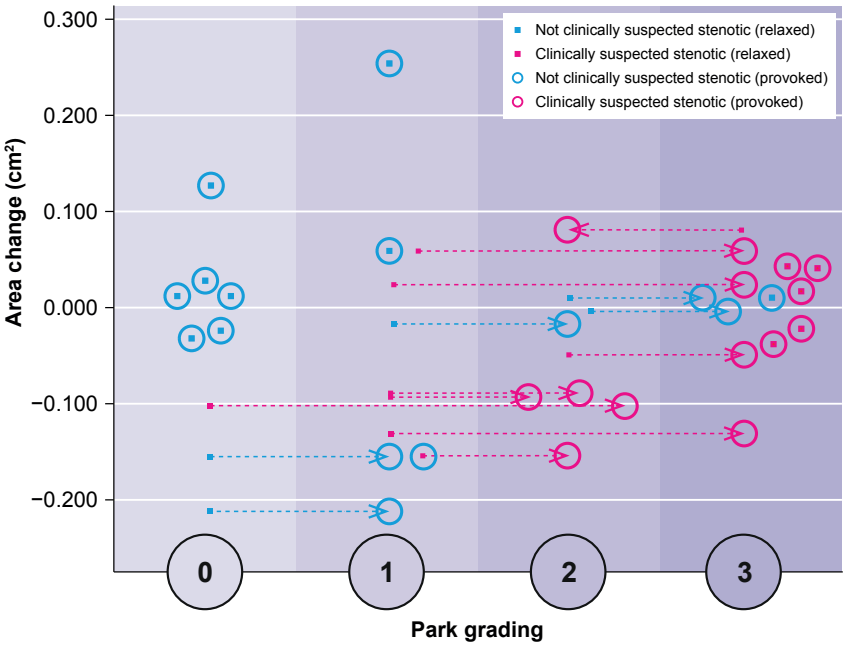

Figure 25 Illustrates the variation in foraminal area (y-axis) in the context of the Park classification (x-axis), which spans from 0 to 3. Foramina identified on the referral MRI as potentially stenotic are indicated with red dots, and those without such suspicion are indicated with blue dots. The red circles indicate the post-provocation classification of foramina initially suspected of foraminal stenosis, while the blue circles indicate the classification of foramina not suspected of stenosis.

Aligned with the alterations in the Park gradings during provocation, the Kim gradings of the foramina also changed. All foramina were evaluated as grade 2 during provocation, marking an increase of 1 to 2 grades compared to in a relaxed state, as depicted in Figure 26.

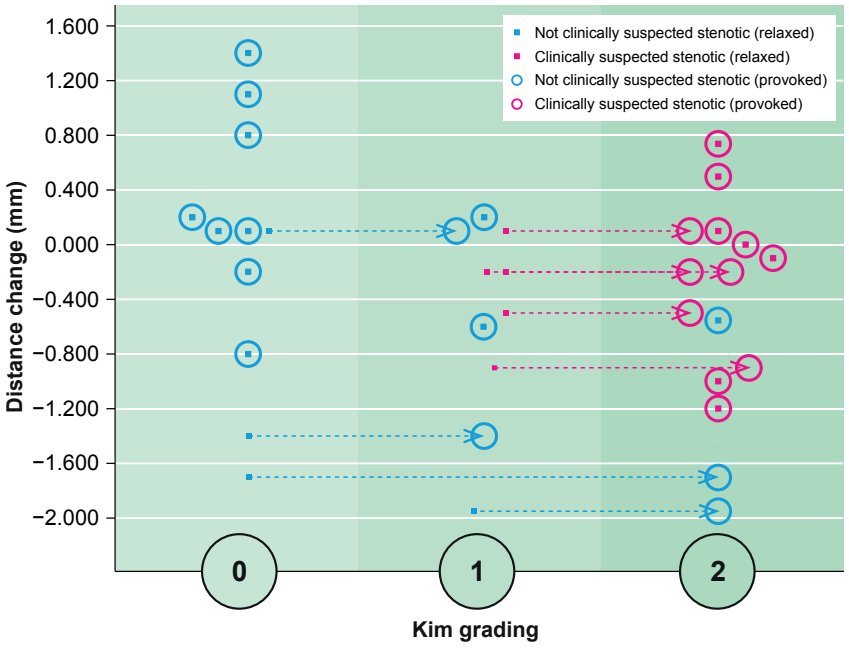

Figure 26 Presents the changes in the foraminal cross-distance (y-axis) mapped against the Kim classification (x-axis), which ranges from 0 to 2. The foramina categorized as suspected stenotic based on MRI findings at the time of referral are represented by red dots, while those considered non-stenotic are represented by blue dots. Post provocation, the red circles indicate the classifications of the foramina previously deemed as potentially stenotic, and the blue circles indicate the classifications of the non-stenotic foramina.

Quantitative measures: The measured changes in foraminal area and cross-distance after conducting the simulated Spurling test were not statistically significant. No statistically significant differences were identified when comparing relaxed and provocation measurements, both in foramina suspected of stenosis and in those not suspected. The foramina that were clinically suspected of stenosis presented with lower area and cross-distance values both before and after provocation. The measured values are presented in Figure 27.

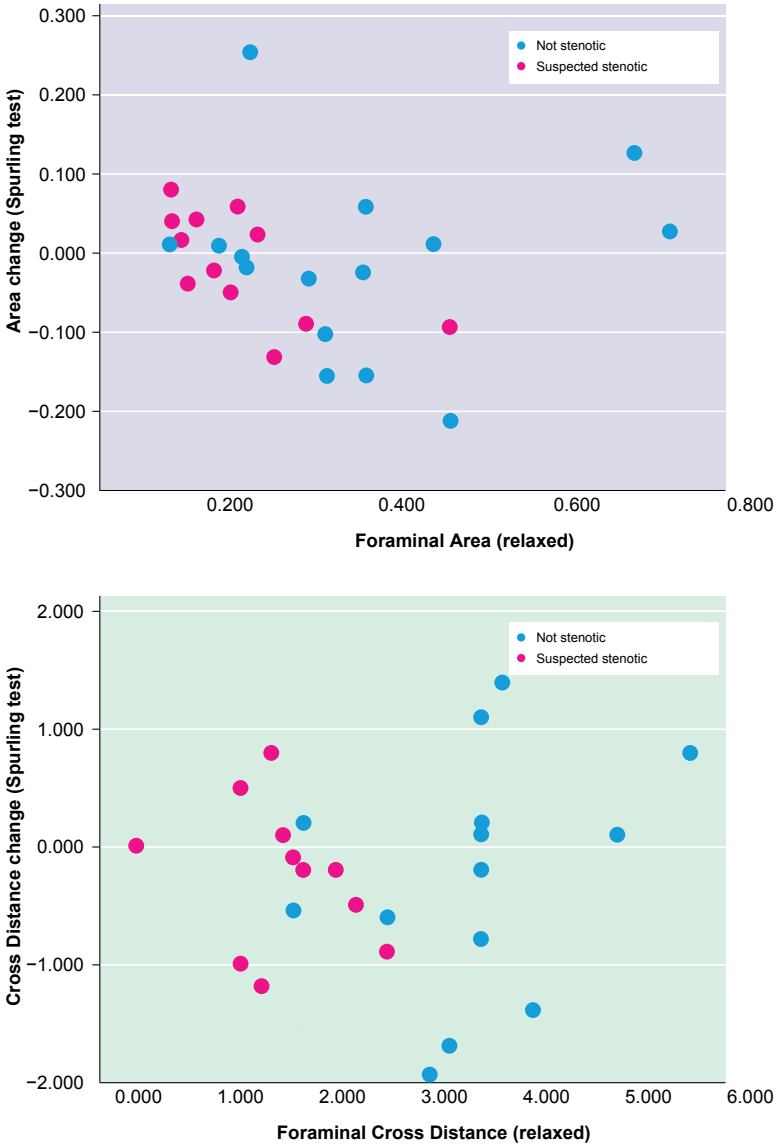

Figure 27 The upper graphic shows the variations in foraminal area after conducting the simulated Spurling test, plotted on the y-axis against the baseline foraminal area on the x-axis. In the corresponding lower graphic, the changes in the cross-distance are shown on the y-axis as related to the baseline cross-distance on the x-axis. The foramina that are clinically suspected of contributing to radiculopathy, as determined from the referral MRI, are indicated with red dots, while those not suspected of clinical significance are indicated with blue dots.

Foraminal Changes Relative to Disc Degeneration: Foramina adjacent to mildly degenerated discs (Pfirrmann grades 2 or 3) showed a decrease in size post provocation. Conversely, those near more severely degenerated discs (grades 4 or 5) displayed inconsistent results, underscoring the complexity of degenerative dynamics in foraminal morphology.

Classification related to whether clinically suspected or not: A significant correlation was found between the likelihood of a foramina being classified at a higher grade of stenosis on the Park scale and stenosis being suspected prior to referral, with this probability being 18.6 times greater (p = 0.002). A similar trend was observed for the Kim classification, with the probability increasing by a factor of 19.6 (p = 0.032). There was an evident correlation between the Park and Kim classification levels and the measurements of foraminal area and cross-distance, in both the relaxed and provoked states, indicating strong associations with a p-value of <0.001 for both grading systems.

Study V

Study cohort and baseline data: The investigation involved ten patients and reviewed 30 cervical foramina. The cohort was the same as in Study IV. The baseline data are therefore in accordance with the data presented in Study IV.

ZTE Imaging and CTMA: Following the processing of the ZTE MRI data and their integration into the CTMA software, the images could be visualized transitioning between two positions, as depicted in Figure 28.

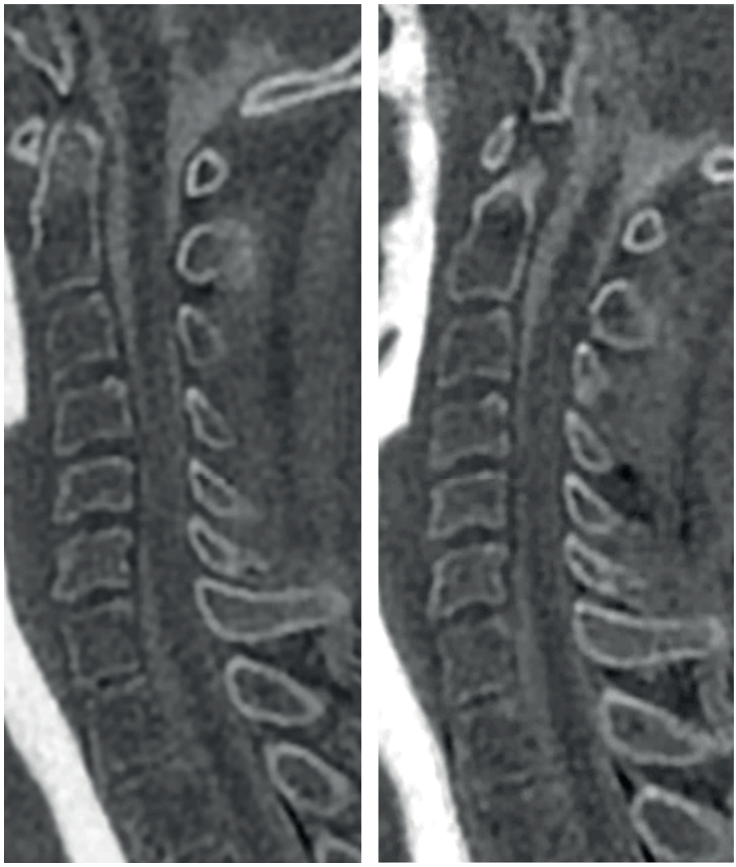

Figure 28 Displays the ZTE MRI images after post-processing for integration with the CTMA software. The image on the left shows the patient in a relaxed state, while the image on the right shows the patient's neck in a simulated Spurling test.

Total rotation and total translation: The analysis of total rotation (Figure 29) and total translation (Figure 30) revealed a decrease in rotational movements from the upper to the lower cervical spine, with the most significant movement at the C4/C5 level. This pattern was consistent irrespective of whether or not the foramina were suspected of being stenotic. The total translation at the top of the foramina displayed variability across the cervical levels, with the greatest range of translation at the C4/C5 level.

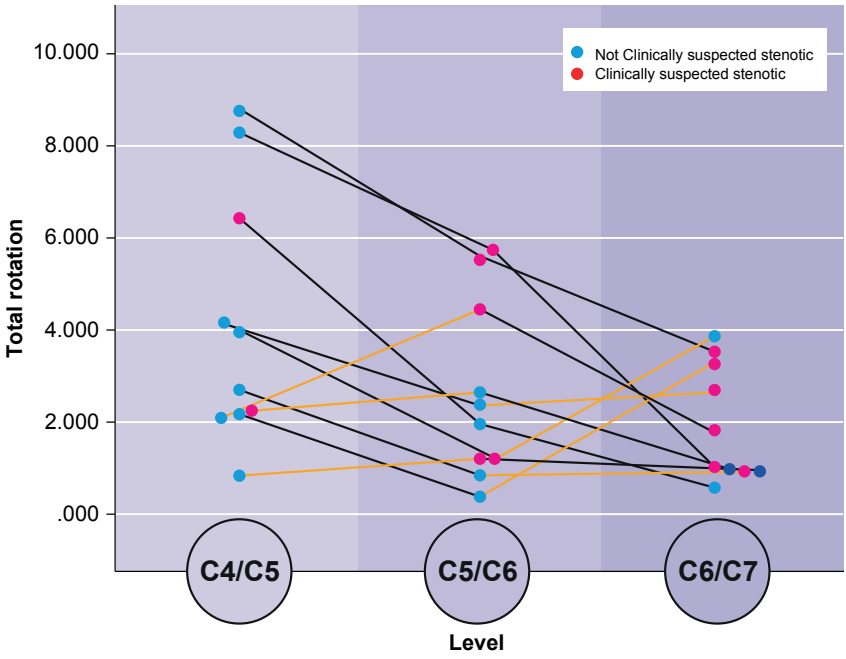

Figure 29 Features a graph depicting the total rotation, measured in degrees on the y-axis, across different levels on the x-axis. Each patient's data points are interconnected by lines. Red dots are used to indicate the levels at which foraminal stenosis is suspected, while blue dots indicate levels considered to be without pathology. Any lines that illustrate an increase in rotation moving from left to right on the graph are highlighted in orange.

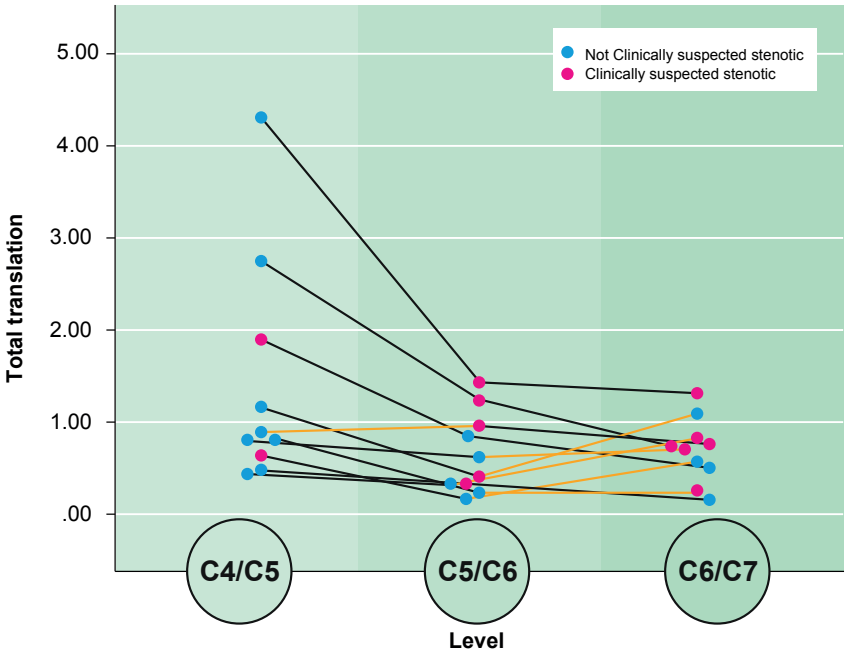

Figure 30 Chart showing the total translation (TT) in degrees on the y-axis against each cervical level on the x-axis. Lines trace the progression of each patient's measurements. Levels at which foraminal stenosis is suspected are indicated with red dots, while blue dots indicate levels at which pathology is not suspected. Lines that incline upward on the chart are highlighted in orange.

Although only slight vertebral movements were induced, nine out of ten patients reported pain consistent with radicular arm pain during the test. No marked differences in motion patterns were detected between foramina initially suspected of being stenotic and those not suspected.

Comparative statistics were performed to evaluate whether there was a pattern among and between the levels classified as suspected of stenosis versus those that were not. No significant statistics could be established, highlighting the variance observed and the small actual movements between the vertebrae during a Spurling test in this limited cohort.

Chapter 10

Discussion

The role of foraminal classification systems

Classification systems play an important role in evidence-based medicine, guiding health policy and aiding the development of clinical practice guidelines.[92] They are commonly utilized in constructing clinical guidelines and assessing research. In the process of narrowing down available classification systems for foraminal stenosis based on MRI (Study I), three crucial elements needed to be present: the images needed to be of sufficient quality; the classification needed to take the neural structures, and not only the bony canal, into account; and, lastly, the system needed to be reliable and validated against symptoms to be clinically relevant. It could be assumed that the ideal classification system would feature precise quantitative metrics with specific thresholds, yet investigations of this approach have revealed considerable challenges. This is due to the considerable variation in the details of size and shape among different humans and especially among ethnic groups.[137] Some expert opinions conclude that a qualitative classification systems are the best approach to grading foraminal stenosis,[138] although the rapid growing development of machine learning and artificial intelligence (AI) may redefine that.[139] As for the currently available classification systems, they need to be validated further to ensure that they are consistent among different users and that the gradings give relevant information that is useful in clinical situations. A few studies have validated the different classification systems and correlated them to symptoms,[108,127-135] and more studies are warranted. A study comparing the Park and Kim systems found that the Park system had a tendency toward higher gradings and higher interrater reliability than the Kim system.[131,140] Furthermore, a modification has been suggested for the Kim system so that it better correlates with symptoms.[128] The modified Kim and Park systems were shown to have a high correlation to clinical manifestations. [131] In the lumbar spine, validating research has been conducted, and the correlation with symptoms has also been confirmed.[132,134]

One step further toward additional validation was taken in our Study V, in which a significant correlation was observed between the classification of foraminal stenosis in initial referral MRI scans and the new relaxed MRI scans, using the Park and Kim classification systems. Images taken during provocation revealed even higher Park and Kim scores, underscoring the reliability of these classifications, and further suggesting the clinical value of provoked-position imaging for accurate diagnosis.[95,126]

The lumbar spine under axial loading

The published article (Study II) on axial loading of the lumbar spine using MRI provides an important addition to our current understanding of lumbar spinal diagnostics.[141,142] Recent studies have further explored the diagnostic value of axial loading in MRI, particularly in assessing lumbar foraminal stenosis and its impact on treatment decisions. Sehic A. et al.[143] have shown that axial-loaded MRI can reveal morphological changes in all segments of the lumbar spine, emphasizing the findings of our current study. Furthermore, Zhong et al.[144] have shown that when analyzing images obtained with and without axial loading, the observed variances across different spinal levels imply a greater likelihood of underestimating nerve root compromise at the L3/L4 and L4/L5 levels compared with the L5/S1 level. In comparison with axial compression, there are further studies demonstrating that spinal extension can lead to reductions in foraminal height, width, and area.[145,146] While upright MRI, in which patients sit or stand during imaging, seems like an optimal investigation method, it has limitations in terms of image quality and accessibility.[147,148] The potential clinical value from the broader perspective of lumbar disorders has been demonstrated by Kanno H. et al.,[149] showing increased spondylolisthesis, decreased dural sac size, and worsened symptoms during axial loading. Another study of the clinical relevance of axial loading during MRI demonstrated changed treatment plans and surgical decisions based on this diagnostic meth-

odology.[142] The application of axial loading in MRI offers a more realistic representation of spinal conditions under physiological stress, potentially unmasking pathologies such as foraminal stenosis or nerve root impingement. Patients who display clear symptoms and clinical findings of nerve root affection without any abnormality in the MRI may benefit from imaging during axial loading. This may help uncover the possible dynamic characteristics of foraminal stenosis, particularly in cases involving conditions such as facet cysts.[150] Axial loading may thereby enhance the correlation between clinical symptoms and radiological findings, aiding in more accurate diagnosis and more effective treatment planning. Another aspect is the possible use of a foraminal classification system (i.e., the Lee system)[93] in conjunction with axial, loading as demonstrated in Study II. Our study showed that 25% of the foramina changed in grading, either increasing or decreasing, after the load was applied. However, the technique poses challenges, such as the need for specialized equipment, potential patient discomfort, and the requirement for experienced radiologists to interpret the images accurately. Altogether, the addition of axial loading during MRI can provide valuable information for the more accurate understanding and possibly treatment of foraminal stenosis in the lumbar spine.

Imaging of the cervical spine during provocation

The DMRICS was introduced in Study III and tested on ten healthy volunteers. The development of the DMRICS was a challenging task, requiring numerous iterations of a few different prototypes. The first prototype used a soft helmet with the hydraulics exerting pulling forces at the four corners. This design was abandoned early on because of problems with expanding air bubbles in the cylinders and hoses leading to uncontrolled reduced forces. Therefore, a rigid helmet was designed with a ball-in-socket concept for the connection with the cylinders delivering pushing forces instead. This eliminated the air bubble problem but instead introduced a problem of instability in the lateral plane. This

problem was solved with a redesign of the connections between the helmet and top plate, including stabilizing pieces on both sides of the helmet. The final prototype proved to be well tolerated by both healthy volunteers and patients with known symptomatic cervical foraminal stenosis. The device was reliable in performing a simulated Spurling test in all cases. Images taken during such a test demonstrated measurable and significant foraminal alterations. This was in concordance with Bartlett et al.,[151] who observed variations in cervical foraminal properties when contrasting the normal supine position with cervical spine extension. Their assessment involved MRI, CT, and CT myelography, noting a constriction of foramina during extension. Another study by Liu et al.[152] identified a considerable augmentation in foraminal area and height under varying degrees of axial traction during MRI. Meanwhile, Muhle et al.[98] found significant alterations in foraminal size on oblique sagittal MRI with the head in extension and ipsilateral rotation, leading to a reduction in foraminal size. Takasaki et al. [119] found changes in the cervical intervertebral foramen during the Spurling test in a manner similar to the current study, but without using a device to control the forces. No foraminal classification systems were used in this study since it examined healthy volunteers and not patients with suspected foraminal stenosis.

In Study IV, on patients with known symptomatic cervical foraminal stenosis, a more clinically realistic approach to the Spurling test was adopted. This was implemented by progressively adjusting the head and cervical positions of patients to replicate the clinical procedure and then pausing for image acquisition once the patient expressed radiculopathy or discomfort. Parameters of NDI and concordant arm pain were collected, further aligning the study with practical clinical utility. Our study demonstrated both increases and decreases in foraminal areas after compression, highlighting the complexity of changes in foraminal properties under these conditions. The findings of varied foraminal properties following controlled compression align with previous research.[119] The observed increase and decrease in some foramina

during provocation are likely due to the variability in the Instantaneous center of rotation (ICR) of a spinal segment, influenced by factors such as the degree of disc degeneration.[153] This may also support the Kirkaldy-Willis theory claiming that there is a part of the degeneration process that is more unstable before it ends up in a fused rigid state.[154] Interestingly, the patients in Study IV demonstrated a significant increase in the qualitative gradings of foraminal stenosis (according to the Park and Kim systems).[94,95] The differences in the biomechanical properties of the discs due to varying degrees of degeneration might account for this, with potential changes in foraminal shape rather than area in patients with more degeneration. The present study noted that foramina adjacent to discs with lower Pfirrmann grades showed a reduction in area and cross-distance following a simulated Spurling test, while foramina next to higher-grade discs showed mixed results. This aligns with findings in the lumbar spine, where more degenerated segments exhibited a smaller range of motion than did less degenerated segments.[155] These findings suggest that disc degeneration may influence the quantitative measurement of foraminal changes in patients, but that qualitative grading systems may overcome that and enable the detection of clinically relevant changes in functional positions.

2D or 3D MRI volume sequences?

MRI acquisitions can be performed in two dimensions (2D) or three dimensions (3D), each serving unique purposes and offering different advantages.[156]

2D MRI acquisitions produce images in two planes: axial, sagittal, or coronal. These images are like slices through the body, providing high-resolution views of a specific area of interest. The advantage of 2D imaging is the speed of acquisition, which is particularly beneficial for patients who might struggle to remain still for long periods, such as children or those in discomfort. Quick scanning times also

reduce the likelihood of motion artifacts, ensuring clearer images. On the other hand, 3D MRI acquisitions capture volumetric data, which can be reconstructed to produce images in any plane after the initial scan.[156] This method involves acquiring a block of tissue data, which allows for more complex post-processing and the ability to reconstruct images with various orientations without the need for additional scanning. The main drawback of 3D MRI is typically longer scan times, which can increase the risk of motion artifacts if the patient moves during the procedure. Recent findings suggest that 3D imaging sequences could offer comparable, or in some cases superior, clinical utility compared with traditional methods. [90,157]

The use of 2D MRI sequences in Study II was identified as a limitation. At this stage of the thesis and during the current circumstances, the lack of 3D volume sequences was identified as a limitation, referring to the benefits that Yamada et al.[158] expanded on. It is important to notice that the Japanese research team primarily emphasized the use of the coronary view, which is generally not used in standard clinical practice by spine surgeons. As for assessing the foramina in the lumbar spine, the sagittal view is considered perhaps the most important image plane, which is why this limitation may not be particularly significant. Notably, Wahezi et al.[159] identified a slight limitation when assessing more than one (optimally angled) foramina per 2D image stack. According to this observation, the absolute optimal view angle is specific per foramina, which is logical and probably true, but the question is how important it is in the clinical reality when investigating the lumbar spine.

In the imaging of cervical foramina the optimal angle is approximately 45 degrees from the sagittal plane, but with some variation.[91] In Study III we therefore chose a T2-weighted volume sequence when obtaining images of the cervical spine during a simulated Spurling test. The images came out with clinically acceptable quality but had some limitations regarding the resolution in order to keep the scanning time to a minimum (3 min). This could lead to measurement

challenges, which can be noted in the somewhat lower ICC values obtained in our studies (Table 7).

Study IV included patients with known cervical pathologies and intermittent radiculopathy. We knew that a minimal scanning time was of the essence in this setup, but even more that the image quality needed to be the best possible to detect very subtle foraminal changes. A newly released software update (SW 29.1) from General Electric (Waukesha, WI, USA) became available at the time of the study start; it was only applicable using 2D image stacks, but with very thin image slices at high resolution. After considering all options, we decided to use this latest software. To make sure that the optimal angle was chosen, at least three of the authors were present at the time of scanning to agree on the placement and angle of the chosen 2D stack of images capturing the oblique sagittal plane. These stacks are 2D but can tolerate a reconstruction to some extent (limited to the total volume of the captured stack), which was utilized when the images were analyzed.

Advancements in the utility of spinal imaging technology

Recently, the ZTE MRI protocols have become increasingly significant, particularly for their potential in orthopedic clinical applications due to their CT-like imaging capabilities.[160] These protocols are advantageous in pre-surgical planning as they provide crucial information (i.e., regarding bone structure) while allowing for image acquisition alongside standard MRI in a single session without subjecting patients to radiation, unlike CT scans.[87] However, the major limitation of ZTE MRI is that its resolution does not match that of conventional CT. Ongoing research is assessing the diagnostic efficacy of ZTE MRI,[161] with the goal of reducing reliance on CT scans for certain diagnoses and pre-surgical preparations, thus saving resources and minimizing patient exposure to radiation.

Radio Stereometric Analysis (RSA) has long been a technique for precisely measuring bone movements between radiological exams, and it is a well-established method for a variety of orthopedic applications, including spinal assessments.[162] RSA has predominantly been employed to track the movements and positional changes of implants and joint prostheses over a period of time.[163] It has been established as an exceptionally precise method for measuring the micromotions of these implants.[164,165] However, RSA is invasive. With advanced computing power becoming more accessible and affordable, there has been a shift towards using computer software for exact comparisons between two sets of images. CTMA by Sectra® represents such a development, and published evidence is accumulating as to its accuracy and non-invasive advantages compared with RSA.[166-168] In our research, CTMA is combined with ZTE MRI, enhancing the approach by further reducing patient exposure to radiation hopefully without necessarily compromising on accuracy.

Study V found distinct movements in the examined mid and lower cervical spine segment levels during the simulated Spurling test using ZTE and Sectra® CTMA. The greatest movement of the three examined segments occurred at the C4/5 level, followed by C5/C6, with minimal movement at C6/C7. Despite minimal vertebral movements, nine out of ten patients experienced arm pain during the test, suggesting that even small changes in foraminal stenosis can cause symptoms. Notably, translations of less than 1 mm were enough to induce radiculopathy. This highlights the advantages of a very accurate methodology to be able to detect such small but yet clinically significant changes.

Overall, the innovative use of ZTE imaging and CTMA software produced findings suggesting this to be a useful tool for improving our understanding of cervical spine dynamics. Combining these techniques with the DMRICS device may provide a comprehensive analysis of conditions in the cervical spine. Utilizing these methods

in tandem could be particularly advantageous for evaluating patients considered for interventions such as disc prosthesis and spinal fusion. This integrated approach has the potential to significantly enhance the diagnosis, treatment, and postoperative care of individuals with cervical spine disorders.

Clinical value

MRI in functional positions offers a promising avenue for improving diagnostic accuracy for foraminal stenosis, especially in patients with position-dependent symptoms. In the lumbar spine, the axial loading may aid in unmasking foraminal stenosis that only produces symptoms in a standing or ambulant situation. In the cervical spine, a simulated Spurling test could be clinically valuable for patient cases with intermittent arm radiculopathy when standard supine MRI fails to conclusively diagnose foraminal stenosis. The method is not presently proposed as a primary diagnostic tool for cervical foraminal stenosis but rather as an adjunct in ambiguous cases. For instance, when multiple foramina exhibit moderate stenosis and the specific levels responsible for symptoms are uncertain, this could impact the selection of appropriate treatment.[151] MRI in functional positions aims to refine diagnostic accuracy in clinical practice. Finally, the use of classification systems to grade foraminal stenosis may be beneficial to a greater extent than first anticipated. Using them in combination with imaging in functional positions is an approach that may support the use of classification systems even more, as shown in Study IV.

Value in research

This thesis lays out the tools for evaluating foraminal stenosis by exploring the literature on validated classification systems. Furthermore, dynamic imaging of the lumbar spine validates previous

studies and sheds light on where the method could be of clinical use. The DMRICS is an innovative approach to dynamic imaging of the cervical spine, offering possibilities for many other research questions, diagnoses, and patient groups.

While the techniques and methods have inherent limitations and challenges, their potential benefits in clinical practice are significant, warranting continued exploration and refinement.

Ethical considerations in imaging in functional positions and diagnosis

There is an ethical dilemma in balancing the need for accurate diagnosis with the need to minimize patient exposure to complicated potentially painful examination procedures. Physicians must weigh the benefits of precise imaging against the potential risks of aggravating patient symptoms.

Patients must be adequately informed of the risks and benefits of spinal imaging procedures. Obtaining informed consent in research studies has not only a legal dimension but also an ethical one, ensuring that patients are empowered to make decisions about their own healthcare. The use of advanced imaging technologies in conjunction with equipment to put the patient in a functional position may also increase the costs. Ethical considerations may therefore also arise regarding the allocation of healthcare resources, especially in settings with limited funding or access to technology. Before adopting new techniques/methods there is a need to consider whether the potential benefits of advanced imaging justify its costs. The increased sensitivity of advanced imaging and accessory technical solution can further lead to overdiagnosis and subsequent overtreatment, which may not always benefit the patient. In the case of both the Dynawell® and DMRICS, the goal is the opposite. Here the goal is to reduce

overtreatment by fine tuning the diagnostics, reducing the extent of surgical interventions.

The use of ZTE MRI in clinical imaging introduces important ethical considerations, particularly in balancing patient safety against diagnostic efficacy. While CT scans remain the gold standard for bony evaluation due to their superior resolution and faster scanning times, they involve exposure to ionizing radiation. This exposure is a significant ethical concern, especially for patients needing frequent scans or for vulnerable populations such as children. In contrast, ZTE MRI, though it may not match the resolution and speed of CT, offers a radiation-free alternative for visualizing bony structures. This feature is crucial in minimizing patient exposure to radiation. Another benefit of ZTE is that it can be done in the same session as the standard MRI, removing the effort of an extra examination for the patient. While ZTE MRI may present challenges in terms of cost and accessibility and may not always replace CT in situations requiring the highest resolution, its use can be valuable in reducing cumulative radiation exposure for patients, thereby upholding ethical standards in healthcare, but more validating studies are warranted.

There should be equal access to high-quality imaging and diagnostic services for all patients, regardless of socioeconomic status or geographic location. Ethical considerations include addressing disparities in healthcare access and striving to provide reasonable care.

There is a risk of becoming overly dependent on technology for diagnosis, potentially undermining the importance of clinical evaluation and history-taking. Physicians must balance the use of technology against their clinical judgment and expertise. The use of advanced imaging must not replace the valuable interaction between physician and patient. Ethical practice involves maintaining this relationship and using advanced imaging as a tool to enhance, rather than replace, physical clinical investigations.

Chapter 11

Limitations

Limitations of the systematic review (Study I)

The reported systematic review may be limited by only searching the English literature. The focus of this thesis is on MRI, so potentially relevant classifications based on CT have been overlooked.

Limitations of MRI in functional positions (Studies II–V)

Generalizability: Studies II–V have a limitation in terms of generalizing their results to the general population. Study II investigated a cohort of patients with LBP without any radiculopathy and studies III–V had a limited number of patients included in the two cohorts.

Statistical power: The small cohorts in the last three studies limit the statistical power to detect possibly significant foraminal changes.

Technical and practical challenges: Implementing MRI in functional positions, especially with devices such as the DMRICS, may involve technical complexities and require additional training for operators. It also introduces practical challenges, such as longer scan times and the need for patient cooperation during positional changes.

Measurement challenges: Quantifying small anatomical features such as nerve roots and foramina on MRIs can be challenging, not only due to their small size but also because of the subtle motions that occur at degenerated foramina in functional positions. The resolution of the images directly limits their accuracy in measuring these small structures in a consistent way. Partial volume effects and the exact angle of the measured MRI plane are also in play, posing possible intrinsic measuring errors.

Interpretation and standardization issues: Consistency in interpreting dynamic MRI images can be challenging, as it requires radiolo-

gists who are familiar with positional variations in spinal anatomy. The standardization of measurement techniques and criteria across different healthcare settings remains an area for further development.

Cost and accessibility: Advanced imaging techniques in functional positions may be more costly than traditional MRI, potentially limiting their widespread use and accessibility in different healthcare settings.

Chapter 12

Conclusion

The studies conducted as part of this thesis have provided insights into the evaluation of MRI and the utility of MRI in functional positions for diagnosing foraminal stenosis.

Study I
Three validated classification systems for cervical or lumbar foraminal stenosis were identified and found to display moderate to high reliability and feasibility in clinical settings, though their clinical validity remains underexplored.

Study II
The application of axial load to the lumbar spine during MRI acquisition in patients with LBP produced a significant mean reduction in foraminal area and alterations of foraminal classifications in 25% of all examined foramina.

Study III
The introduction of the DMRICS for simulating a Spurling test in the cervical spine was demonstrated, and the device was well tolerated by the healthy pilot subjects. The DMRICS proved to be user-friendly and reliable for simulating functional positions during MRI scans, achieving clinically acceptable image quality for all but one foramina. A significant increase in cervical angle and a reduction in the foraminal cross-distance during provocation were demonstrated.

Study IV
The enrolled patients were able to perform the MRI scan in a relaxed position followed by image acquisition in a Spurling position during the triggered arm radiculopathy, resulting in images of clinically acceptable quality in nine out of ten cases. The classification gradings of foraminal stenosis increased significantly during the provocation.

Study V
It was feasible to create a non-ionizing investigative method for

analyzing the cervical spine movement using ZTE images obtained with the DMRICS, in conjunction with CTMA. The study demonstrated greater movement in the examined C4/C5 segments than in the next two lower levels.

Chapter 13

Future perspectives

Given the evolving evidence, future research should focus on optimizing protocols for imaging in functional positions—specifically, positions that patients might assume during activities that provoke their symptoms—and on exploring their utility across different patient populations, as opposed to the traditional relaxed supine positioning. Studies comparing functional positions in MRI with other diagnostic modalities, such as CT scans when appropriate, could further establish their role in clinical practice.

The MRI represents a marvel of medical engineering, standing at the forefront of a rapidly advancing field. I am convinced that we are just scratching the surface of its potential capabilities. Notably, the development of new MRI protocols that capture chemical activity in various tissues is attracting significant interest. This innovative approach holds the promise of not only visualizing but also comprehending the intricate functionalities or potential dysfunctions within the tissues under examination. What if we could visualize nerve activity during image acquisition in routine clinical diagnosis work? The combination of new MRI protocols and acquisition in functional positions (when nerve symptoms are triggered) could revolutionize our understanding of human biology and make way for groundbreaking diagnostic and therapeutic techniques.

Additionally, the integration of dynamic imaging with machine learning offers a promising avenue for enhancing image processing. By leveraging AI, researchers could potentially develop systems that automatically adjust for variations in patient positioning, reduce noise, and even predict the progression of conditions such as foraminal stenosis. Perhaps AI-assisted MRI protocols could aid in the pinpointing of symptomatic nerve roots. This could possibly lead to high-definition MRI images that provide clearer, more actionable insights without the need for increased radiation exposure.

The findings of this thesis pave the way for further research on opti-

mizing MRI techniques in functional positions, particularly regarding standardizing and broadening clinical applications. Future studies should focus on larger patient cohorts and diverse clinical scenarios to validate and refine these imaging methodologies. They could potentially incorporate new advanced MRI sequences and AI, so that in the future we might get a closer look at the actual function of a nerve root, for example. These advances could revolutionize the quality and diagnostic utility of MRI, contributing to more precise and personalized medical care.

Acknowledgements

I would like to thank the **University of Gothenburg,** specifically the **Sahlgrenska Academy, the Institution for Clinical Sciences,** and the **Department of Orthopaedics** represented by **Anders Björkman** and **Ola Rolfson** for the opportunity to conduct this thesis research.

I would also like to thank the **Orthopaedic Clinic** represented by **Anna Nilsdotter** and **the section for Spine and Tumor Surgery** represented by **Christina Berger.**

The completion of this thesis is a testament to the collaborative spirit and exceptional abilities of my colleagues. I extend my deepest appreciation **to all** who have contributed to this project, whether directly involved or indirectly influencing its trajectory from afar.

Helena Brisby, my extraordinary supervisor. I am immensely grateful for your ability to recognize my enthusiasm for medical engineering and that you were able to inspire and guide the creation of the DMRICS. Your talents for perceiving the potential in people, sparking a passion for discovery, envisioning innovation within clinical practice, outstandingly reviewing scientific manuscripts, and being a dependable guide in challenging surgical situations, are truly remarkable. You are a living legend!

Hanna Hebelka, my co-supervisor, and invaluable source of support. Almost quicker to answer an email than Google can finish a search. Always there with clear answers and structure in everything you do. Thank you for making me feel that I was your most important adept.

Kerstin Lagerstrand, co-supervisor and engineering inspiration. You are a professor in its essence, brilliant and smart with solutions to every possible obstacle. Thank you for always questioning my line of thought in a kind but sharp way, challenging every detail of the project, leading up to this thesis.

Kajsa Rennerfelt, for all your hard work in being one of the co-authors. We miss you a lot as a colleague and spine surgeon at Sahlgrenska!

Elin Stävlid, for your meticulous MRI measurements and for being a resource as a co-author.

Pär-Arne Svensson, for being a world-class captain of the MRI scanners during the studies and for showing up during evenings and weekends to get the work done.

Emilia Palmér, your effort and expertise in adapting the MRI images for use with the CTMA software are greatly appreciated.

Aldina Pivodic, for your brilliance in statistics, making sure we got all the numbers in place, using the right statistical models.

Tor Åge Myklebust, for lending us your fantastic skills in statistics.

Helena Lund Maaninka, for fixing all the practical hiccups with Heroma, Lingmerths, and the list goes on...

Cina Holmer, for being a steady source of knowledge in the academic world during the first part of my time as a doctoral student.

Nurses and nursing assistants, I am grateful for your dedication and assistance with the workflow of my academic work in the clinic

Healthy volunteers and patients, we thank you for placing your trust in our research and for participating in our endeavor to advance human knowledge just a little bit further.

Pontus Andersson, for your outstanding talent in making almost every illustration I have used in both the published papers and this thesis.

Anna Orosz, for your support in guiding me through the academic maze to reach the goal of writing, publishing, and defending my thesis.

Thomas Hutchins, my father, and role model. You are the mastermind behind the construction of the DMRICS, building and programming it from the bottom up. I remember how you tweaked the force-measuring programming just two weeks before your body could not take more of the spreading cancer. I miss you more than words can say.

Caroline Hutchins, my incredible sister and friend for all your skills and knowledge of 3D modeling and technical design, leading up to the DMRICS. Your dedication to the project has been invaluable.

Carlos Ribeiro, my brilliant brother-in-law for your amazing talent in technical design and solution-finder in times of despair when building the DMRICS.

Peter Nyberg, you are the true master of strong leadership and an incredible spine surgeon. Thank you for hiring me for the Spine Surgery team at Sahlgrenska.

Mikael Klingenstierna, the lighthouse of the Spine Surgery unit at Sahlgrenska, the navigation beacon in stormy weather. Thank you for being my friend and keeping me on course!

Joel Beck, thank you for teaching and giving me hints in all the small things along the journey of becoming a better spine surgeon, just by getting to know you. You truly make Sahlgrenska a better place to work at.

Vojtech Capek, my "roommate" at Elevhemmet, thank you for being my spine surgery hero, teaching and guiding me tremendously in both theory and in the operating room.

Olof Westin, for being such an invaluable college and friend. You truly lead by example which has made a huge impact on me.

Per Wessberg, my revered senior colleague and a star in the field of spine surgery, I am deeply grateful for the privilege of being mentored by you in surgical practices. Thank you for also being such a good friend sharing laughs and great conversations.

Adad Baranto, I am grateful for the opportunity to learn from you. Your surgical talent is exceptional, and your proficiency in optimizing efficiency across all facets of our professional life is truly admirable.

Peter Kores, a precious colleague and friend. You are one of the most talented teachers in surgical skills out there. You taught me endless small tips and tricks in the operating room that I highly value in pretty much every surgery I perform.

Catharina Parai, for your friendship and support in the everyday working life. I appreciate all the hours we spent together in the operating room. You taught me so many things. I'm so grateful that you decided to join the Sahlgrenska Spine Surgery crew.

Hosam Shamma, I appreciate your contribution to the Sahlgrenska Spine Surgery team, bringing with you a wealth of knowledge as a neurosurgeon, along with your incredible stories from your experiences.

Jesper Hallsten, for being a great friend and colleague. It is always a joy to perform surgery together, but also to just talk about life, video games and other toys for big boys.

Sara Brandt-Knutsson, thank you for delivering exceptional medical care at the Sahlgrenska Spine Surgery unit. Your consistent professionalism, complemented by your cheerful attitude and contagious laughter, truly enhances our workplace.

Christina Berger, thank you for being such a fantastic person to be around. Your humble approach to everything is a true superpower. Thank you for believing in me and giving me the opportunity to become better and grow in the clinic.

Peter Bergh, Mikael Dalén, Sigvard Eriksson, David Wennergren, Marianne Flinck, and Erik Malchau, the superstar tumor surgery team at Sahlgrenska, whom I greatly admire. Thank you for making Elevhemmet a better place to be!

Kardo Raouf, thank you for showing me your art of smacking in pedicle screws in a perfect line, like a Boss! We miss you a lot at Sahlgrenska, come back.

Petter Gustafsson, my senior colleague and friend who is the reason I'm performing spine surgery today. Thank you for showing your magic that Easter of 2014 when your discectomy transformed a patient from being bedbound and in unbearable pain to walking out pain-free the following day.

John Eliasson and Anne Garland, for being my shining stars to look up to and learn from during my orthopedic residency in Gotland.

Fredrik Olerud, for being a close friend all the way through. Starting as orthopedic residents on Gotland to living quite far apart but still having precious conversations about work, research, and life.

Erik Elmqvist, for sharing the experience of exploring spine surgery together as junior residents on Gotland.

Tönu Saartok, for being a true leader and chief by example. Thank you for planting the seed of pursuing academics back in Gotland during the early days of my medical career.

Anne-Marie Hutchins, my mother and constant supporter and encourager in every situation. Your ability to always make me feel special and good enough whatever I dig myself into. Thank you for taking care of Alfred and the kids at least one day every week during my parental leave, making it possible to write this thesis.

Lena Carlsson, my mother-in-law, for your all-round knowledge and ability to discuss any subject. I think you still have more university credits than I do even after this thesis. Thank you for your tremendous help with looking after the children during times when the family and work schedules were challenging to coordinate.

Alfred Hutchins, my youngest son, for being such a fantastic little person to hang out with during the writing of the larger part of this thesis. Sitting by my side, almost always smiling when I'm at the computer or on the phone trying to get my research together.

Oscar Hutchins, my middle son, giving me the opportunity to leave what I'm doing to jump into your world of imagination, playing with Lego or driving Traxxas. You can really make me feel like I'm a child again with all the playful joy you bring to the family.

Noel Hutchins, my oldest son, for always being so curious about everything in life including my research. It is unbelievable how I can have advanced conversations with you on technical and clinical subjects. You are a brilliant little guy, but I can still beat you in Grand Turismo 7!

Emma Hutchins, my wonderful wife, and partner in life. Thank you for always believing in me. Thank you for sharing your time with me every day, making me feel that I need nothing more in life.

References

1 Devereaux, M. W. Anatomy and Examination of the Spine. *Neurologic Clinics* **25**, 331-351 (2007). https://doi.org:https://doi.org/10.1016/j.ncl.2007.02.003

2 Bellitti, R., Testini, V., Piccarreta, R. & Guglielmi, G. Imaging of the Ageing Spine. *Current radiology reports (Philadelphia, PA)* **9** (2021). https://doi.org:10.1007/s40134-021-00388-0

3 Yousem, D. M., Atlas, S. W., Goldberg, H. I. & Grossman, R. I. Degenerative narrowing of the cervical spine neural foramina: evaluation with high-resolution 3DFT gradient-echo MR imaging. *AJNR. American journal of neuroradiology* **12**, 229 (1991).

4 Yamada, K. *et al.* Lumbar foraminal stenosis causes leg pain at rest. *European spine journal : official publication of the European Spine Society, the European Spinal Deformity Society, and the European Section of the Cervical Spine Research Society* **23**, 504-507 (2014). https://doi.org:10.1007/s00586-013-3055-3

5 Abbed, K. M. & Coumans, J. V. Cervical radiculopathy: pathophysiology, presentation, and clinical evaluation. *Neurosurgery* **60**, S28-34 (2007). https://doi.org:10.1227/01.Neu.0000249223.51871.C2

6 Jenis, G. L. & An, S. H. Spine Update: Lumbar Foraminal Stenosis. *Spine* **25**, 389-394 (2000). https://doi.org:10.1097/00007632-200002010-00022

7 Choi, Y. K. Lumbar foraminal neuropathy: an update on non-surgical management. *Korean J Pain* **32**, 147-159 (2019). https://doi.org:10.3344/kjp.2019.32.3.147

8 MacDowall, A. *et al.* Artificial disc replacement versus fusion in patients with cervical degenerative disc disease and radiculopathy: a randomized controlled trial with 5-year outcomes. *Journal of Neurosurgery Spine* **30**, 323-331 (2019).

9 Orita, S. *et al.* Lumbar foraminal stenosis, the hidden stenosis including at L5/S1. *European Journal of Orthopaedic Surgery & Traumatology* **26**, 685-693 (2016). https://doi.org:10.1007/s00590-016-1806-7

10 Nicotra, A., Khalil, N. M. & O'Neill, K. Cervical radiculopathy: discrepancy or concordance between electromyography and magnetic resonance imaging? *Br J Neurosurg* **25**, 789-790 (2011). https://doi.org:10.3109/02688697.2011.594189

11 Panjabi, M. The Stabilizing System of the Spine. Part I. Function, Dysfunction, Adaptation, and Enhancement. *Journal of spinal disorders* **5**, 383-389; discussion 397 (1993). https://doi.org:10.1097/00002517-199212000-00001

12 Bogduk, N. Functional anatomy of the spine. *Handb Clin Neurol* **136**, 675-688 (2016). https://doi.org:10.1016/b978-0-444-53486-6.00032-6

13 Pope, M. H. Biomechanics of the lumbar spine. *Ann Med* **21**, 347-351 (1989). https://doi.org:10.3109/07853898909149219

14 Holck, P. [Anatomy of the cervical spine]. *Tidsskr Nor Laegeforen* **130**, 29-32 (2010). https://doi.org:10.4045/tidsskr.09.0296

15 Waxenbaum, J. A., Reddy, V. & Futterman, B. in *StatPearls* (StatPearls Publishing. Copyright © 2023, StatPearls Publishing LLC., 2023).

16 Raj, P. P. Intervertebral disc: anatomy-physiology-pathophysiology-treatment. *Pain Pract* **8**, 18-44 (2008). https://doi.org:10.1111/j.1533-2500.2007.00171.x

17 Bogduk, N. & Endres, S. M. (Elsevier/Churchill Livingstone New York, New York, 2005).

18 Adams, M. A. & Roughley, P. J. What is intervertebral disc degeneration, and what causes it? *Spine* **31**, 2151-2161 (2006). https://doi.org:10.1097/01.brs.0000231761.73859.2c

19 Tonetti, J. *et al.* Morphological cervical disc analysis applied to traumatic and degenerative lesions. *Surgical and Radiologic Anatomy* **27**, 192-200 (2005). https://doi.org:10.1007/s00276-004-0309-0

20 White, A. A. & Panjabi, M. M. *Clinical biomechanics of the spine*. 2nd edn, XXIII, 722 str. : ilustr. ; 27 cm. (J. B. Lippincott Philadelphia, 1990).

21 Netter, F. H., Hansen, J. T. & Lambert, D. R. *Netter's clinical anatomy*. 1st edn, ix, 668 pages : illustrations ; 23 cm (Icon Learning Systems Carlstadt, N.J., 2005).

22 Cramer, G. D., Darby, S. A. & Cramer, G. D. *Clinical anatomy of the spine, spinal cord, and ANS*. Third Edition edn, (Elsevier, 2014).

23 Fisicaro, M. D., Grauer, J. N., Beiner, J. M., Kwon, B. K. & Vaccaro, A. R. in *Core Knowledge in Orthopaedics: Spine* (ed Alexander R. Vaccaro) 1-13 (Mosby, 2005).

24 Jaumard, N. V., Welch, W. C. & Winkelstein, B. A. Spinal facet joint biomechanics and mechanotransduction in normal, injury and degenerative conditions. *J Biomech Eng* **133**, 071010 (2011). https://doi.org:10.1115/1.4004493

25 Pal, G. P., Routal, R. V. & Saggu, S. K. The orientation of the articular facets of the zygapophyseal joints at the cervical and upper thoracic region. *J Anat* **198**, 431-441 (2001). https://doi.org:10.1046/j.1469-7580.2001.19840431.x

26 Hartman, J. Anatomy and clinical significance of the uncinate process and uncovertebral joint: A comprehensive review. *Clin Anat* **27**, 431-440 (2014). https://doi.org:10.1002/ca.22317

27 Kapetanakis, S. & Gkantsinikoudis, N. Anatomy of lumbar facet joint: a comprehensive review. *Folia Morphologica* **80**, 799-805 (2021). https://doi.org:10.5603/FM.a2020.0122

28 Mohanty, S. P., Pai Kanhangad, M., Kamath, S. & Kamath, A. Morphometric study of the orientation of lumbar zygapophyseal joints in a South Indian population. *Journal of Orthopaedic Surgery* **25**, 2309499017739483 (2017). https://doi.org:10.1177/2309499017739483

29 Caridi, J. M., Pumberger, M. & Hughes, A. P. Cervical radiculopathy: a review. *Hss j* **7**, 265-272 (2011). https://doi.org:10.1007/s11420-011-9218-z

30 Neumann, D. A. *Kinesiology of the musculoskeletal system : foundations for physical rehabilitation*. (First edition. St. Louis : Mosby, [2002] ©2002, 2002).

31 O'Sullivan, P. B. Masterclass. Lumbar segmental 'instability': clinical presentation and specific stabilizing exercise management. *Manual Therapy* **5**, 2-12 (2000). https://doi.org:https://doi.org/10.1054/math.1999.0213

32 Richardson, C. A. *et al.* The Relation Between the Transversus Abdominis Muscles, Sacroiliac Joint Mechanics, and Low Back Pain. *Spine* **27** (2002).

33 Solomonow, M., Zhou, B.-H., Harris, M., Lu, Y. & Baratta, R. V. The Ligamento-Muscular Stabilizing System of the Spine. *Spine* **23** (1998).

34 Cavanaugh, J. M., Ozaktay, A. C., Yamashita, H. T. & King, A. I. Lumbar facet pain: Biomechanics, neuroanatomy and neurophysiology. *Journal of Biomechanics* **29**, 1117-1129 (1996). https://doi.org:https://doi.org/10.1016/0021-9290(96)00023-1

35 Dowdell, J., Kim, J., Overley, S. & Hecht, A. Biomechanics and common mechanisms of injury of the cervical spine. *Handb Clin Neurol* **158**, 337-344 (2018). https://doi.org:10.1016/b978-0-444-63954-7.00031-8

36 Van Mameren, H., Drukker, J., Sanches, H. & Beursgens, J. Cervical spine motion in the sagittal plane (I) range of motion of actually performed movements, an X-ray cinematographic study. *Eur J Morphol* **28**, 47-68 (1990).

37 Buonocore, E., Hartman, J. T. & Nelson, C. L. Cineradiograms of cervical spine in diagnosis of soft-tissue injuries. *Jama* **198**, 143-147 (1966). https://doi.org:10.1001/jama.198.1.143

38 Penning, L. Differences in anatomy, motion, development and aging of the upper and lower cervical disk segments. *Clin Biomech (Bristol, Avon)* **3**, 37-47 (1988). https://doi.org:10.1016/0268-0033(88)90124-6

39 Amevo, B., Worth, D. & Bogduk, N. Instantaneous axes of rotation of the typical cervical motion segments: II. optimization of technical errors. *Clin Biomech (Bristol, Avon)* **6**, 38-46 (1991). https://doi.org:10.1016/0268-0033(91)90040-w

40 Amevo, B., Worth, D. & Bogduk, N. Instantaneous axes of rotation of the typical cervical motion segments: a study in normal volunteers. *Clin Biomech (Bristol, Avon)* **6**, 111-117 (1991). https://doi.org:10.1016/0268-0033(91)90008-e

41 van Mameren, H., Sanches, H., Beursgens, J. & Drukker, J. Cervical spine motion in the sagittal plane. II. Position of segmental averaged instantaneous centers of rotation--a cineradiographic study. *Spine* **17**, 467-474 (1992). https://doi.org:10.1097/00007632-199205000-00001

42 Nowitzke, A., Westaway, M. & Bogduk, N. Cervical zygapophyseal joints: geometrical parameters and relationship to cervical kinematics. *Clin Biomech (Bristol, Avon)* **9**, 342-348 (1994). https://doi.org:10.1016/0268-0033(94)90063-9

43 Hartvigsen, J. *et al.* What low back pain is and why we need to pay attention. *Lancet* **391**, 2356-2367 (2018). https://doi.org:10.1016/s0140-6736(18)30480-x

44 Clarençon, F., Law-Ye, B., Bienvenot, P., Cormier, É. & Chiras, J. The Degenerative Spine. *Magn Reson Imaging Clin N Am* **24**, 495-513 (2016). https://doi.org:10.1016/j.mric.2016.04.008

45 Wong, S. H., Chiu, K. Y. & Yan, C. H. Review Article: Osteophytes. *J Orthop Surg (Hong Kong)* **24**, 403-410 (2016). https://doi.org:10.1177/1602400327

46 Kalichman, L. & Hunter, D. J. Diagnosis and conservative management of degenerative lumbar spondylolisthesis. *Eur Spine J* **17**, 327-335 (2008). https://doi.org:10.1007/s00586-007-0543-3

47 Belavy, D. L. *et al.* Pain sensitivity is reduced by exercise training: Evidence from a systematic review and meta-analysis. *Neurosci Biobehav Rev* **120**, 100-108 (2021). https://doi.org:10.1016/j.neubiorev.2020.11.012

48 Parkinson, J. An essay on the shaking palsy. 1817. *J. Neuropsychiatry Clin. Neurosci.* **14**, 223-236; discussion 222 (2002). https://doi.org:10.1176/jnp.14.2.223

49 Mansfield, M., Smith, T., Spahr, N. & Thacker, M. Cervical spine radiculopathy epidemiology: A systematic review. *Musculoskeletal care* (2020). https://doi.org:10.1002/msc.1498

50 Radhakrishnan, K., Litchy, W. J., O'Fallon, W. M. & Kurland, L. T. Epidemiology of cervical radiculopathy: A population-based study from Rochester, Minnesota, 1976 through 1990. *Brain (London, England : 1878)* **117**, 325-335 (1994). https://doi.org:10.1093/brain/117.2.325

51 Matsumoto, M. *et al.* MRI of cervical intervertebral discs in asymptomatic subjects. *Journal of bone and joint surgery. British volume* **80**, 19-24 (1998). https://doi.org:10.1302/0301-620X.80B1.0800019

52 Hoy, D. *et al.* The global burden of neck pain: estimates from the Global Burden of Disease 2010 study. *Annals of the rheumatic diseases* **73**, 1309-1315 (2014). https://doi.org:10.1136/annrheumdis-2013-204431

53 V., P. New conceptions in the pathogenesis of sciatic pain. *Lancet 2:53–60* (1927).

54 Yamada, K. *et al.* Lumbar foraminal stenosis causes leg pain at rest. *European Spine Journal* **23**, 504-507 (2014).

55 Rao, R. Neck Pain, Cervical Radiculopathy, and Cervical Myelopathy: Pathophysiology, Natural History, and Clinical Evaluation. *Journal of bone and joint surgery. American volume* **84**, 1872-1881 (2002). https://doi.org:10.2106/00004623-200210000-00021

56 Woods, B. I. & Hilibrand, A. S. Cervical Radiculopathy: Epidemiology, Etiology, Diagnosis, and Treatment. *Clinical Spine Surgery* **28**, E251-E259 (2015). https://doi.org:10.1097/bsd.0000000000000284

57 Tawa, N., Rhoda, A. & Diener, I. Accuracy of clinical neurological examination in diagnosing lumbo-sacral radiculopathy: a systematic literature review. *BMC Musculoskelet Disord* **18**, 93 (2017). https://doi.org:10.1186/s12891-016-1383-2

58 Dützmann, S., Fernandez, R. & Rosenthal, D. [Thoracic spinal stenosis : Etiology, pathogenesis, and treatment]. *Orthopade* **48**, 844-848 (2019). https://doi.org:10.1007/s00132-019-03731-8

59 Zimmerman, B. & Hubbard, J. B. in *StatPearls* (StatPearls Publishing. Copyright © 2024, StatPearls Publishing LLC., 2024).

60 Whitwam, J. G. Classification of peripheral nerve fibres. An historical perspective. *Anaesthesia* **31**, 494-503 (1976). https://doi.org:10.1111/j.1365-2044.1976.tb12354.x

61 Navarro, X., Vivó, M. & Valero-Cabré, A. Neural plasticity after peripheral nerve injury and regeneration. *Progress in Neurobiology* **82**, 163-201 (2007). https://doi.org:https://doi.org/10.1016/j.pneurobio.2007.06.005

62 Campbell, W. W. Evaluation and management of peripheral nerve injury. *Clinical Neurophysiology* **119**, 1951-1965 (2008). https://doi.org:https://doi.org/10.1016/j.clinph.2008.03.018

63 Coleman, M. P. & Freeman, M. R. Wallerian degeneration, wld(s), and nmnat. *Annu Rev Neurosci* **33**, 245-267 (2010). https://doi.org:10.1146/annurev-neuro-060909-153248

64 Lundborg, G. Intraneural microcirculation. *Orthop Clin North Am* **19**, 1-12 (1988).

65 Brushart, T. M. Motor axons preferentially reinnervate motor pathways. *J Neurosci* **13**, 2730-2738 (1993). https://doi.org:10.1523/jneurosci.13-06-02730.1993

66 Viikari-Juntura, E., Porras, M. & Laasonen, E. M. Validity of clinical tests in the diagnosis of root compression in cervical disc disease. *Spine* **14**, 253-257 (1989). https://doi.org:10.1097/00007632-198903000-00003

67 Tong, H. C., Haig, A. J. & Yamakawa, K. The Spurling test and cervical radiculopathy. *Spine (Phila Pa 1976)* **27**, 156-159 (2002). https://doi.org:10.1097/00007632-200201150-00007

68 Thoomes, E. J. *et al.* Value of physical tests in diagnosing cervical radiculopathy: a systematic review. *Spine J* **18**, 179-189 (2018). https://doi.org:10.1016/j.spinee.2017.08.241

69 Jones, S. J. & Miller, J. M. M. in *StatPearls* (StatPearls Publishing. Copyright © 2022, StatPearls Publishing LLC., 2022).

70 Lee, M. W. L., McPhee, R. W. & Stringer, M. D. An evidence-based approach to human dermatomes. *Clinical anatomy (New York, N.Y.)* **21**, 363-373 (2008). https://doi.org:10.1002/ca.20636

71 Magee, D. J. *Musculoskeletal rehabilitation series* (Elsevier Saunders St. Louis, Missouri, St. Louis, Missouri, 2014).

72 Apelby-Albrecht, M. *et al.* Concordance of upper limb neurodynamic tests with medical examination and magnetic resonance imaging in patients with cervical radiculopathy: a diagnostic cohort study. *J Manipulative Physiol Ther* **36**, 626-632 (2013). https://doi.org:10.1016/j.jmpt.2013.07.007

73 Gumina, S., Carbone, S., Albino, P., Gurzi, M. & Postacchini, F. Arm Squeeze Test: a new clinical test to distinguish neck from shoulder pain. *Eur Spine J* **22**, 1558-1563 (2013). https://doi.org:10.1007/s00586-013-2788-3

74 Shabat, S., Leitner, Y., David, R. & Folman, Y. The correlation between Spurling test and imaging studies in detecting cervical radiculopathy. *J Neuroimaging* **22**, 375-378 (2012). https://doi.org:10.1111/j.1552-6569.2011.00644.x

75 Shah, K. C. & Rajshekhar, V. Reliability of diagnosis of soft cervical disc prolapse using Spurling's test. *Br J Neurosurg* **18**, 480-483 (2004). https://doi.org:10.1080/02688690400012350

76 Camino Willhuber, G. O. & Piuzzi, N. S. in *StatPearls* (StatPearls Publishing. Copyright © 2022, StatPearls Publishing LLC., 2022).

77 Berthelot, J. M. *et al.* Inadequacies of the Lasègue test, and how the Slump and Bowstring tests are useful for the diagnosis of sciatica. *Joint Bone Spine* **88**, 105030 (2021). https://doi.org:10.1016/j.jbspin.2020.06.004

78 Majlesi, J., Togay, H., Ünalan, H. & Toprak, S. The Sensitivity and Specificity of the Slump and the Straight Leg Raising Tests in Patients With Lumbar Disc Herniation. *JCR: Journal of Clinical Rheumatology* **14** (2008).

79 Ekedahl, H., Jönsson, B., Annertz, M. & Frobell, R. B. Accuracy of Clinical Tests in Detecting Disk Herniation and Nerve Root Compression in Subjects With Lumbar Radicular Symptoms. *Arch Phys Med Rehabil* **99**, 726-735 (2018). https://doi.org:10.1016/j.apmr.2017.11.006

80 Hesselink, J. R. Spine imaging: history, achievements, remaining frontiers. *AJR Am J Roentgenol* **150**, 1223-1229 (1988). https://doi.org:10.2214/ajr.150.6.1223

81 Hounsfield, G. N. Computerized transverse axial scanning (tomography). 1. Description of system. *Br J Radiol* **46**, 1016-1022 (1973). https://doi.org:10.1259/0007-1285-46-552-1016

82 Kretzschmar, K. Degenerative diseases of the spine. The role of myelography and myelo-CT. *Eur J Radiol* **27**, 229-234 (1998). https://doi.org:10.1016/s0720-048x(97)00170-8

83 Lauterbur, P. C. Image Formation by Induced Local Interactions: Examples Employing Nuclear Magnetic Resonance. *Nature* **242**, 190-191 (1973). https://doi.org:10.1038/242190a0

84 Vargas, M. I., Boto, J. & Meling, T. R. Imaging of the spine and spinal cord: An overview of magnetic resonance imaging (MRI) techniques. *Revue Neurologique* **177**, 451-458 (2021). https://doi.org:https://doi.org/10.1016/j.neurol.2020.07.005

85 Chavhan, G. B. Appropriate selection of MRI sequences for common scenarios in clinical practice. *Pediatric Radiology* **46**, 740-747 (2016). https://doi.org:10.1007/s00247-016-3556-4

86 Guadilla, I., Calle, D. & López-Larrubia, P. in *Preclinical MRI: Methods and Protocols* (eds María Luisa García Martín & Pilar López Larrubia) 89-101 (Springer New York, 2018).

87 Weiger, M., Brunner, D. O., Dietrich, B. E., Müller, C. F. & Pruessmann, K. P. ZTE imaging in humans. *Magn Reson Med* **70**, 328-332 (2013). https://doi.org:10.1002/mrm.24816

88 Botchu, R., Bharath, A., Davies, A. M., Butt, S. & James, S. L. Current concept in upright spinal MRI. *European Spine Journal* **27**, 987-993 (2018). https://doi.org:10.1007/s00586-017-5304-3

89 Delfaut, E. M. *et al.* Fat suppression in MR imaging: techniques and pitfalls. *Radiographics* **19**, 373-382 (1999). https://doi.org:10.1148/radiographics.19.2.g99mr03373

90 Lee, S. *et al.* MRI of the lumbar spine: comparison of 3D isotropic turbo spin-echo SPACE sequence versus conventional 2D sequences at 3.0 T. *Acta Radiol* **56**, 174-181 (2015). https://doi.org:10.1177/0284185114524196

91 Kintzele, L., Rehnitz, C., Kauczor, H. U. & Weber, M. A. Oblique Sagittal Images Prevent Underestimation of the Neuroforaminal Stenosis Grade Caused by Disc Herniation in Cervical Spine MRI. *Rofo: Fortschritte auf dem Gebiete der Rontgenstrahlen und der Nuklearmedizin* **190**, e2 (2018).

92 Irving, M., Eramudugolla, R., Cherbuin, N. & Anstey, K. J. A Critical Review of Grading Systems: Implications for Public Health Policy. *Evaluation & the Health Professions* **40**, 244-262 (2016). https://doi.org:10.1177/0163278716645161

93 Lee, S. *et al.* A practical MRI grading system for lumbar foraminal stenosis. *AJR. American journal of roentgenology* **194**, 1095 (2010). https://doi.org:10.2214/AJR.09.2772

94 Park, H. J. *et al.* A practical MRI grading system for cervical foraminal stenosis based on oblique sagittal images. *Br J Radiol* **86**, 20120515 (2013). https://doi.org:10.1259/bjr.20120515

95 Kim, S. *et al.* A New MRI Grading System for Cervical Foraminal Stenosis Based on Axial T2-Weighted Images. *Korean J Radiol* **16**, 1294-1302 (2015). https://doi.org:10.3348/kjr.2015.16.6.1294

96 Lord, E. L. *et al.* Kinetic magnetic resonance imaging of the cervical spine: a review of the literature. *Global Spine J* **4**, 121-128 (2014). https://doi.org:10.1055/s-0034-1375563

97 Michelini, G. *et al.* Dynamic MRI in the evaluation of the spine: state of the art. *Acta Biomed* **89**, 89-101 (2018). https://doi.org:10.23750/abm.v89i1-S.7012

98 Muhle, C., Resnick, D., Ahn, J. M., Südmeyer, M. & Heller, M. In Vivo Changes in the Neuroforaminal Size at Flexion-Extension and Axial Rotation Of The Cervical Spine In Healthy Persons Examined Using Kinematic Magnetic Resonance Imaging. *Spine* **26**, e287-e293 (2001). https://doi.org:10.1097/00007632-200107010-00013

99 Axel, L. Biomechanical dynamics of the heart with MRI. *Annu Rev Biomed Eng* **4**, 321-347 (2002). https://doi.org:10.1146/annurev.bioeng.4.020702.153434

100 Kolcun, J. P., Chieng, L. O., Madhavan, K. & Wang, M. Y. The Role of Dynamic Magnetic Resonance Imaging in Cervical Spondylotic Myelopathy. *Asian Spine J* **11**, 1008-1015 (2017). https://doi.org:10.4184/asj.2017.11.6.1008

101 Wildermuth, S. *et al.* Lumbar spine: quantitative and qualitative assessment of positional (upright flexion and extension) MR imaging and myelography. *Radiology* **207**, 391-398 (1998). https://doi.org:10.1148/radiology.207.2.9577486

102 Baker, M. A. & MacKay, S. Please be upstanding - A narrative review of evidence comparing upright to supine lumbar spine MRI. *Radiography (Lond)* **27**, 721-726 (2021). https://doi.org:10.1016/j.radi.2020.11.003

103 Klein, H. M. Low-Field Magnetic Resonance Imaging. *Rofo* **192**, 537-548 (2020). https://doi.org:10.1055/a-1123-7944

104 Cheng, K. Recent progress in high-resolution functional MRI. *Curr Opin Neurol* **24**, 401-408 (2011). https://doi.org:10.1097/WCO.0b013e3283489711

105 Marques, J. P., Simonis, F. F. J. & Webb, A. G. Low-field MRI: An MR physics perspective. *J Magn Reson Imaging* **49**, 1528-1542 (2019). https://doi.org:10.1002/jmri.26637

106 Benoist, M. Natural history of the aging spine. *Eur Spine J* **12 Suppl 2**, S86-89 (2003). https://doi.org:10.1007/s00586-003-0593-0

107 Efstathiou, M. A., Stefanakis, M., Savva, C. & Giakas, G. Effectiveness of neural mobilization in patients with spinal radiculopathy: a critical review. *J Bodyw Mov Ther* **19**, 205-212 (2015). https://doi.org:10.1016/j.jbmt.2014.08.006

108 Kim, M. S., Lee, D. G. & Chang, M. C. Outcome of Transforaminal Epidural Steroid Injection According to Severity of Cervical Foraminal Stenosis. *World Neurosurgery* **110**, e398-e403 (2018).

109 Chang, M. C. & Lee, D. G. Outcome of Transforaminal Epidural Steroid Injection According to the Severity of Lumbar Foraminal Spinal Stenosis. *Pain Physician* **21**, 67-72 (2018).

110 Helm, S. *et al.* Transforaminal epidural steroid injections: A systematic review and meta-analysis of efficacy and safety. *Pain Physician* **24(S1)**, 209-232 (2021).

111 Skeppholm, M. *et al.* Artificial disc replacement versus fusion in cervical radiculopathy: is there more to discover? A randomized control trial with 2 years follow-up. *European spine journal* **23**, S547–S548 (2014). https://doi.org:10.1007/s00586-014-3517-2

112 Rossi, V. & Adamson, T. Cervical Spine Surgery: Arthroplasty Versus Fusion Versus Posterior Foraminotomy. *Neurosurg Clin N Am* **32**, 483-492 (2021). https://doi.org:10.1016/j.nec.2021.05.005

113 Özer, A. F. *et al.* Lumbar Foraminal Stenosis Classification That Guides Surgical Treatment. *Int J Spine Surg* **16**, 666-673 (2022). https://doi.org:10.14444/8311

114 Cerezci, O. & Başak, A. T. Importance of Physiotherapy after Lumbar Microdiscectomy. *Turk Neurosurg* **33**, 150-155 (2023). https://doi.org:10.5137/1019-5149.Jtn.40904-22.5

115 Ozkara, G. O. *et al.* Effectiveness of physical therapy and rehabilitation programs starting immediately after lumbar disc surgery. *Turk Neurosurg* **25**, 372-379 (2015). https://doi.org:10.5137/1019-5149.Jtn.8440-13.0

116 Willen, J. & Danielson, B. The diagnostic effect from axial loading of the lumbar spine during computed tomography and magnetic resonance imaging in patients with degenerative disorders. *Spine* **26**, 2607-2614 (2001).

117 Iwata, T. *et al.* In vivo measurement of lumbar foramen during axial loading using a compression device and computed tomography. *J Spinal Disord Tech* **26**, E177-182 (2013). https://doi.org:10.1097/BSD.0b013e318286f635

118 Splendiani, A. *et al.* Magnetic resonance imaging (MRI) of the lumbar spine with dedicated G-scan machine in the upright position: a retrospective study and our experience in 10 years with 4305 patients. *La radiologia medica* **121**, 38-44 (2016). https://doi.org:10.1007/s11547-015-0570-9

119 Takasaki, H. *et al.* The influence of cervical traction, compression, and spurling test on cervical intervertebral foramen size. *Spine* **34**, 1658-1662 (2009).

120 Lee, S. *et al.* A practical MRI grading system for lumbar foraminal stenosis. *AJR. American Journal of Roentgenology* **194**, 1095-1098 (2010).

121 Pfirrmann, C. W. A., Metzdorf, A., Zanetti, M., Hodler, J. & Boos, N. Magnetic Resonance Classification of Lumbar Intervertebral Disc Degeneration. *Spine* **26**, 1873-1878 (2001).

122 Svedmark, P. *et al.* A New CT Method for Assessing 3D Movements in Lumbar Facet Joints and Vertebrae in Patients before and after TDR. *Biomed Res Int* **2015**, 260703 (2015). https://doi.org:10.1155/2015/260703

123 Brodén, C. *et al.* Accuracy and precision of a CT method for assessing migration in shoulder arthroplasty: an experimental study. *Acta Radiol* **61**, 776-782 (2020). https://doi.org:10.1177/0284185119882659

124 Sandberg, O. H. *et al.* Computed tomography-based radiostereometric analysis in orthopedic research: practical guidelines. *Acta Orthop* **94**, 373-378 (2023). https://doi.org:10.2340/17453674.2023.15337

125 Vernon, H. Assessment of Self-Rated Disability, Impairment, and Sincerity of Effort in Whiplash-Associated Disorder. *Journal of Musculoskeletal Pain* **8**, 155-167 (2000). https://doi.org:10.1300/J094v08n01_13

126 Park, H. J. *et al.* A practical MRI grading system for cervical foraminal stenosis based on oblique sagittal images. *British Journal of Radiology* **86**, 20120515 (2013).

127 Kim, W., Ahn, K.-S., Kang, C. H., Kang, W. Y. & Yang, K.-S. Comparison of MRI grading for cervical neural foraminal stenosis based on axial and oblique sagittal images: Concordance and reliability study. *Clinical Imaging* **43**, 165-169 (2017). https://doi.org:10.1016/j.clinimag.2017.03.008

128 Park, H. J. *et al.* Clinical correlation of a new and practical magnetic resonance grading system for cervical foraminal stenosis assessment. *Acta Radiologica* **56**, 727-732 (2015). https://doi.org:10.1177/0284185114537929

129 Lee, K. H. *et al.* Comparison of two MR grading systems for correlation between grade of cervical neural foraminal stenosis and clinical manifestations. *The British Journal of Radiology* **89**, 20150971 (2016). https://doi.org:10.1259/bjr.20150971

130 Park, H. J. *et al.* The Clinical Correlation of a New Practical MRI Method for Grading Cervical Neural Foraminal Stenosis Based on Oblique Sagittal Images. *American Journal of Roentgenology* **203**, 412-417 (2014). https://doi.org:10.2214/AJR.13.11647

131 Lee, J. E. *et al.* Interreader Reliability and Clinical Validity of a Magnetic Resonance Imaging Grading System for Cervical Foraminal Stenosis. *Journal of Computer Assisted Tomography* **41**, 926-930 (2017).

132 Park, H. J. *et al.* Clinical Correlation of a New MR Imaging Method for Assessing Lumbar Foraminal Stenosis. *American Journal of Neuroradiology* **33**, 818 (2012). https://doi.org:10.3174/ajnr.A2870

133 Kang, W. Y. *et al.* Is multidetector computed tomography comparable to magnetic resonance imaging for assessment of lumbar foraminal stenosis? *Acta Radiologica* **58**, 197-203 (2017).

134 Jeong, T. S. *et al.* Correlation between MRI Grading System and Surgical Findings for Lumbar Foraminal Stenosis. *Journal of Korean Neurosurgical Society* **60**, 465-470 (2017).

135 Hofmann, U. K., Keller, R. L., Gesicki, M., Walter, C. & Mittag, F. Interobserver Reliability When Classifying MR Imaging of the Lumbar Spine: Written Instructions Alone Do Not Suffice. *Magnetic Resonance in Medical Sciences* **19**, 207-215 (2020).

136 Hutchins, J. *et al.* Cervical Foraminal Changes in Patients with Intermittent Arm Radiculopathy Studied with a New MRI-Compatible Compression Device. *Journal of Clinical Medicine* **12**, 6493 (2023).

137 Lin, H. H. *et al.* What is the difference in morphologic features of the lumbar vertebrae between Caucasian and Taiwanese subjects? A CT-based study: implications of pedicle screw placement via Roy-Camille or Weinstein method. *BMC Musculoskelet Disord* **20**, 252 (2019). https://doi.org:10.1186/s12891-019-2602-4

138 Andreisek, G. *et al.* Consensus conference on core radiological parameters to describe lumbar stenosis - an initiative for structured reporting. *Eur Radiol* **24**, 3224-3232 (2014). https://doi.org:10.1007/s00330-014-3346-z

139 Laulloo, A., Meacock, J., Currie, S., Leng, J. & Thomson, S. Literature Review of Automated Grading Systems Utilizing MRI for Neuroforaminal Stenosis. *Curr Med Imaging* **19**, 874-884 (2023). https://doi.org:10.2174/1573405618666220628100928

140 Kim, W., Ahn, K. S., Kang, C. H., Kang, W. Y. & Yang, K. S. Comparison of MRI grading for cervical neural foraminal stenosis based on axial and oblique sagittal images: Concordance and reliability study. *Clinical Imaging* **43**, 165-169 (2017).

141 Hansen, B. B. *et al.* Weight-bearing MRI of the Lumbar Spine: Spinal Stenosis and Spondylolisthesis. *Semin Musculoskelet Radiol* **23**, 621-633 (2019). https://doi.org:10.1055/s-0039-1697937

142 Hiwatashi, A. *et al.* Axial Loading during MR Imaging Can Influence Treatment Decision for Symptomatic Spinal Stenosis. *American Journal of Neuroradiology* **25**, 170-174 (2004).

143 Sehic, A. *et al.* Magnetic Resonance Imaging Evaluation of Biomechanical Effects of Axial Loading on the Lumbar Spine. *Acta Inform Med* **30**, 312-317 (2022). https://doi.org:10.5455/aim.2022.30.312-317

144 Zhong, W. M. D. *et al.* In vivo dynamic changes of dimensions in the lumbar intervertebral foramen. *The spine journal* **15**, 1653-1659 (2015). https://doi.org:10.1016/j.spinee.2015.03.015

145 Cha, T. D. *et al.* In Vivo Characteristics of Nondegenerated Adjacent Segment Intervertebral Foramina in Patients With Degenerative Disc Disease During Flexion-Extension. *Spine* **42**, 359-365 (2017). https://doi.org:10.1097/brs.0000000000001758

146 Fujiwara, A., An, H. S., Lim, T. H. & Haughton, V. M. Morphologic changes in the lumbar intervertebral foramen due to flexion-extension, lateral bending, and axial rotation: an in vitro anatomic and biomechanical study. *Spine* **26**, 876-882 (2001). https://doi.org:10.1097/00007632-200104150-00010

147 Kubosch, D. *et al.* The Lumbar Spine as a Dynamic Structure Depicted in Upright MRI. *Medicine (Baltimore)* **94**, e1299 (2015). https://doi.org:10.1097/md.0000000000001299

148 Lang, G. *et al.* Preoperative Assessment of Neural Elements in Lumbar Spinal Stenosis by Upright Magnetic Resonance Imaging: An Implication for Routine Practice? *Cureus* **10**, e2440 (2018). https://doi.org:10.7759/cureus.2440

149 Kanno, H. *et al.* An increase in the degree of olisthesis during axial loading reduces the dural sac size and worsens clinical symptoms in patients with degenerative spondylolisthesis. *Spine J* **18**, 726-733 (2018). https://doi.org:10.1016/j.spinee.2017.08.251

150 Kinder, A. *et al.* Magnetic resonance imaging of the lumbar spine with axial loading: A review of 120 cases. *European journal of radiology* **81**, e561-e564 (2011). https://doi.org:10.1016/j.ejrad.2011.06.027

151 Bartlett, R. J., Hill, C. A., Rigby, A. S., Chandrasekaran, S. & Narayanamurthy, H. MRI of the cervical spine with neck extension: is it useful? *Br J Radiol* **85**, 1044-1051 (2012). https://doi.org:10.1259/bjr/94315429

152 Liu, J. *et al.* Quantitative changes in the cervical neural foramen resulting from axial traction: in vivo imaging study. *The Spine Journal* **8**, 619-623 (2008). https://doi.org:https://doi.org/10.1016/j.spinee.2007.04.016

153 Guo, Z., Cui, W., Sang, D. C., Sang, H. P. & Liu, B. G. Clinical Relevance of Cervical Kinematic Quality Parameters in Planar Movement. *Orthop Surg* **11**, 167-175 (2019). https://doi.org:10.1111/os.12435

154 Yong-Hing, K. & Kirkaldy-Willis, W. The pathophysiology of disc degeneration of the lumbar spine. *Ortho Clin North Am* **14**, 59-64 (1983).

155 Vaisy, M. *et al.* Measurement of Lumbar Spine Functional Movement in Low Back Pain. *The Clinical Journal of Pain* **31**, 876-885 (2015). https://doi.org:10.1097/ajp.0000000000000190

156 Sahr, M., Tan, E. T. & Sneag, D. B. 3D MRI of the Spine. *Semin Musculoskelet Radiol* **25**, 433-440 (2021). https://doi.org:10.1055/s-0041-1731060

157 Barnaure, I., Galley, J., Fritz, B. & Sutter, R. Magnetic resonance imaging in the evaluation of cervical foraminal stenosis: comparison of 3D T2 SPACE with sagittal oblique 2D T2 TSE. *Skeletal Radiol* **51**, 1453-1462 (2022). https://doi.org:10.1007/s00256-022-03988-9

158 Yamada, H. *et al.* Improved accuracy of diagnosis of lumbar intra and/or extra-foraminal stenosis by use of three-dimensional MR imaging: comparison with conventional MR imaging. *Journal of Orthopaedic Science* **20**, 287-294 (2015).

159 Wahezi, S. E. *et al.* MRI and Anatomical Determinants Affecting Neuroforaminal Stenosis Evaluation: A Descriptive Observational Study. *J Pain Res* **15**, 1515-1526 (2022). https://doi.org:10.2147/jpr.S360847

160 Aydıngöz, Ü., Yıldız, A. E. & Ergen, F. B. Zero Echo Time Musculoskeletal MRI: Technique, Optimization, Applications, and Pitfalls. *Radiographics* **42**, 1398-1414 (2022). https://doi.org:10.1148/rg.220029

161 Argentieri, E. C. *et al.* Diagnostic Accuracy of Zero-Echo Time MRI for the Evaluation of Cervical Neural Foraminal Stenosis. *Spine* **43**, 928-933 (2018).

162 Humadi, A., Dawood, S., Halldin, K. & Freeman, B. RSA in Spine: A Review. *Global Spine J* **7**, 811-820 (2017). https://doi.org:10.1177/2192568217701722

163 Bottner, F. *et al.* Radiostereometric Analysis: The Hip. *HSS Journal®* **1**, 94-99 (2005). https://doi.org:10.1007/s11420-005-0114-2

164 Valstar, E. R. *et al.* Guidelines for standardization of radiostereometry (RSA) of implants. *Acta Orthopaedica* **76**, 563-572 (2005). https://doi.org:10.1080/17453670510041574

165 Ten Brinke, B. *et al.* The accuracy and precision of radiostereometric analysis in upper limb arthroplasty. *Acta Orthop* **88**, 320-325 (2017). https://doi.org:10.1080/17453674.2017.1291872

166 Brodén, C., Sandberg, O., Olivecrona, H., Emery, R. & Sköldenberg, O. Precision of CT-based micromotion analysis is comparable to radiostereometry for early migration measurements in cemented acetabular cups. *Acta Orthop* **92**, 419-423 (2021). https://doi.org:10.1080/17453674.2021.1906082

167 Engseth, L. H. W., Schulz, A., Pripp, A. H., Röhrl, S. M. H. & Øhrn, F. D. CT-based migration analysis is more precise than radiostereometric analysis for tibial implants: a phantom study on a porcine cadaver. *Acta Orthop* **94**, 207-214 (2023). https://doi.org:10.2340/17453674.2023.12306

168 Clarke, S. G., Logishetty, K., Halewood, C. & Cobb, J. P. Low dose CT-based spatial analysis (CTSA) to measure implant migration after ceramic hip resurfacing arthroplasty (HRA): A phantom study. *Proc Inst Mech Eng H* **237**, 359-367 (2023). https://doi.org:10.1177/09544119231153905